University of South Bohemia, Faculty of Science
Department of Molecular Biology

Influence of Juvenile Hormone and its Receptors on the Immune system during Metamorphosis of Drosophila melanogaster

Bachelor Thesis

Verena Fettinger
22.5.2020
Supervisor: Marek Jindra, prof. PhD

Fettinger V., 2020: Influence of Juvenile Hormone and its Rezeptors on the Immune system during Metamorphosis of *Drosophila melanogaster*. Bc. Thesis, in English 59 p., Faculty of Science, University of South Bohemia, České Budějovice, Czech Republic.

Annotation:

Juvenile hormone is known to have both immune suppressing and developmental effects in several insect species. During *Drosophila melanogaster* metamorphosis, several events require regulation by JH which is mediated through the JH receptors Methoprene-tolerant (Met*)* and germ cell expressed (Gce*).* This thesis is focused on the effect JH and its receptors have during metamorphosis and whether they can be related to an occurring immune challenge or developmental events.

Declaration:

I hereby declare that I have worked on my bachelor's thesis independently and used only the sources listed in the bibliography.

I hereby declare that, in accordance with Article 47b of Act No. 111/1998 in the valid wording, I agree with the publication of my bachelor thesis, in full to be kept in the Faculty of Science archive, in electronic form in publicly accessible part of the IS STAG database operated by the University of South Bohemia in České Budějovice accessible through its web pages. Further, I agree to the electronic publication of the comments of my supervisor and thesis opponents and the record of the proceedings and results of the thesis defense in accordance with the aforementioned Act No. 111/1998. I also agree with the comparison of the text of my thesis with the Theses.cz thesis database operated by the National Registry of University Theses and a plagiarism detection system.

Ampflwang, 21.5.2020

....

Verena Fettinger

Acknowledgements

I would like to express my utmost appreciation to my supervisor Dr. Marek Jindra for his time, guidance and advice throughout the laboratory and analysis process and for his trust in my responsibility and autonomy regarding the experimental execution. It was extremely educational and rewarding to work in your laboratory.

Furthermore, I want to thank my friends and family for their support and kindness any time of the day I needed it.

Abstract

Juvenile hormone (JH) has both immune suppressive and developmental effects in *Drosophila melanogaster*. In this thesis we hypothesize that during metamorphosis the histolysis of tissue and extensive remodelling of the flies' body lead to an immune challenge. The role of JH during metamorphosis could therefore be both developmental and immune regulating.

JH signals are mediated by the JH receptors Gce and Met. While the functionalities of Gce and Met often overlap, functional Gce is the more important JH receptor for immune regulation. The immune system of *Drosophila melanogaster* reacts with the expression of Antimicrobial peptides (AMPs) to immune challenges. Expression of AMPs during metamorphosis is altered through JH-dependent regulation, but whether AMPs are solely part of immunity or also play a developmental role in the pupal stage is still unknown. Furthermore, the role both JH receptor genes Gce and Met play during metamorphosis was investigated.

For this thesis, experiments have been designed to show the impact of the presence or absence of JH and its receptors on the immune response represented by AMP mRNA expression during metamorphosis. Q-RT-PCR was used to create AMP mRNA profiles in the background of unfunctional JH signalling due to one mutated JH receptor, with *w gce^{2,5k}* and *w Met^{27}* lacking Gce or Met, respectively. The results were then compared to the natural AMP expression obtained from the *y w* control genotype.

Analysis of the results showed that the hypothesis we started this thesis with was mostly confirmed. The prevailing trend of immune gene upregulation in the absence of JH signalling, particularly in the genotype *w gce^{2,5k}* lacking a functional Gce receptor, and downregulation by JHa, indicate the immune suppressive function of JH during metamorphosis mainly mediated by Gce. Not all investigated AMP genes follow the same trend, which may reflect their different and more complicated regulation. Some genes were found to be more sensitive to the loss of the JH receptor Met, some more sensitive to the loss of Gce.

Regulation of AMP expression and therefore immune suppression by JH and its receptors Gce and Met could be associated with several timepoints during metamorphosis correlating with lysis and abdominal restructuring events.

Inhalt

Introduction

For this thesis, the Immune response during *Drosophila melanogaster* metamorphosis and its dependence on JH and the JH receptor *Met* and *gce* are of utmost interest. In the following chapters, details to their functionality in the organism *Drosophila melanogaster* are presented.

Development of *Drosophila melanogaster*

Drosophila melanogaster is one of the most popular organisms for research in the fields of genetics and developmental biology. As a holometabolous insect, *D. melanogaster* have larval, pupal, and adult developmental stages. When fruit flies are not prior killed for research, they have a life span of approximately 10 weeks. (Tyler, 2000)
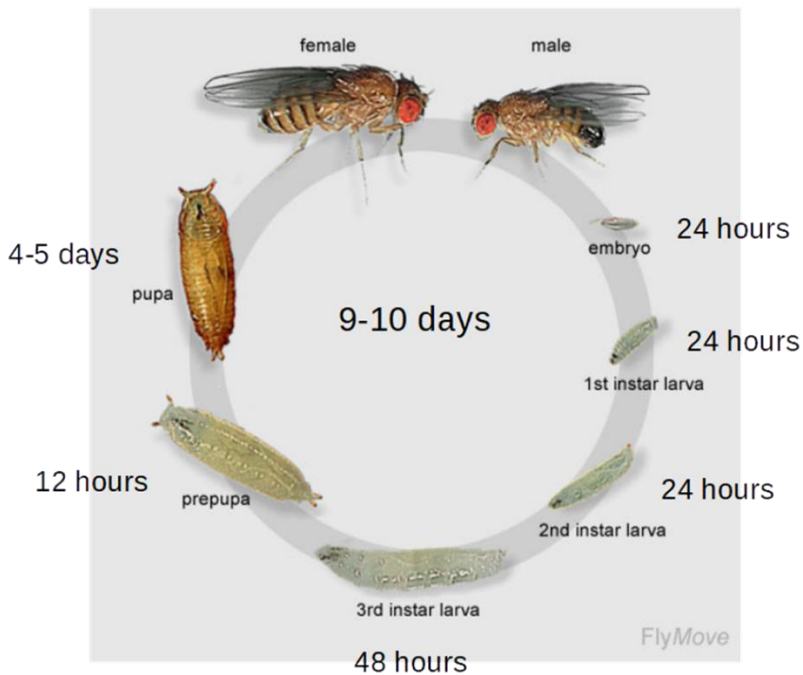

Figure 1: Life cycle of Drosophila melanogaster, picture adapted from (University of Washington, kein Datum)

The life cycle of the fruit fly is shown in figure 1. Females lay their eggs after mating with first instar larvae emerging from them after 22-24 hours. After feeding for 25 hours, first instar larvae molt into second instar larvae. Molting into third instar larvae takes place after 24 hours of feeding. The third instar larvae then, after it stored enough energy by feeding, find themselves a spot to undergo pupation. The molting of the third instar larvae into pupae takes place after approximately 30 hours. In the early stages of this stationary form, the pupa has a yellowish-white colour and is called a prepupa or white pupa. With time the pupa turns increasingly brown and dark. During the pupal stage the larvae undergo metamorphosis into the adult form (imago), after approximately 4 days the adult fly emerges from its pupal case. (Tyler, 2000)

Pupation

When the third instar larva has fed enough and is ready for pupation it leaves the feeding medium (cornmeal-molasses-agar-mixture) it has up until then been living in and wanders to find a suitable spot for pupation on a firm surface. Its body shortens and movement ceases to a halt. Transformation of the cuticle to a puparium follows. In the beginning, the puparium is soft and its colour is white but then turns

increasingly harder and brownish over time. Shortly after puparium formation, the larva molts for a fourth time and thereby detaches itself from the inside of the puparium. Then Metamorphosis of the larva to the adult begins. (Tyler, 2000)

Metamorphosis

During metamorphosis most larval tissue is lysed, with only some larval organs being preserved. The larval nervous system is not degraded but undergoes significant reconstruction. Malpighian tubules, which are excretory structures, fat bodies and gonads are not lysed as well. The larval tissue undergoes histolysis during the prepupal and early pupal stage while adult tissue grows from differentiating imaginal cells. The new adult tissue is formed from two sets of cells, imaginal discs and histoblasts. These cells are present within the larva in all instar stages but stay undifferentiated, mitotic cells. During the pupal stage these cells start differentiating and form the adult tissue which replaces the degraded larval structures. (Tyler, 2000) (Jiang, et al., 1997)

Metamorphosis in *Drosophila melanogaster* is dependent on regulation by the steroid hormone 20-hydroxyecdysone. A pulse of ecdysone at the end of larval development leads to puparium formation and starts prepupal development. 10 hours later another ecdysone pulse triggers pupation and therefore defines the transition from prepupa to pupa. Pulses of 20-hydroxyecdysone direct the destruction of larval tissue and its replacement with adult tissue. The histolysis of larval tissue is a programmed cell death response triggered stage-specifically by the hormone. Cell death is induced by expression of the *Drosophila* death genes *reaper* (*rpr*) and *defective* (*hid*) while anti-cell death genes like *diap2* are suppressed. Ecdysone has both positive and negative regulatory functions on different genes. The regulation of cell death by ecdysone is both highly stage- and tissue-specific. (Jiang, et al., 1997)

Timeline

For this thesis, what happens in the pupa during metamorphosis at the timepoints 0h, 6h, 18h, 24h, 30h, 36h, 42h, 48h, 60h and 72h after puparium formation is investigated. The stages and the corresponding timepoints at which they have been observed are shown in figure 2-5. The numbers next to each developmental event in figures 3-5 correspond to the stages P1-15 described in figure 2. For this thesis stages P1-10 from are of interest.

At the beginning of the prepupal stage (0h after WP stage) the posterior spiracles and ridge between anterior spiracles tan orange, the puparium turns brown and the male gonads become less distinct. 6h after WP stage, the contractions of the dorsal medial abdomen stop, the ridge of the operculum becomes distinct and the puparium separates from the underlying epidermis, starting at the anterior end. At 18h and 24h after WP stage, a pair of white Malpighian tubules becomes visible dorsally in the abdomen and they become prominent and green. 30h after WP stage, the white Malpighian tubules still becomes visible dorsally in the abdomen and they become prominent and green, while at the same time the dark green "yellow body" appears between the anterior end of the Malpighian tubules segments, mid-dorsally at the anterior end of the abdomen. 36h after WP stage, the white Malpighian tubules still becomes visible dorsally in the abdomen and they become prominent and green, while the dark green "yellow body" appears and the transparent pupal cuticle separates from the underlying epidermis, starting on the posterior end. 42h after WP stage the same events as at 36h are taking place. 48h after WP stage, the white Malpighian tubules finish becoming visible dorsally in the abdomen and green and the transparent pupal cuticle is still separating from the underlying epidermis. 72h after WP stage the eyes become a pale pink. (Bainbridge & Bownes, 1981)

The onset of metamorphosis is signalled by an ecdysone pulse that targets intersegmental muscles. Motoneurons directing larval proleg muscles degenerate, and the salivary glands of drosophila are also believed to start disintegrating at this time. Abdominal muscles and the larval salivary glands undergo histolysis shortly after pupation. An ecdysone pulse at approximately 10h after puparium formation targets the salivary glands. The cells are fully lysed after 15h after puparium formation. (Jiang, et al., 1997)

Dramatic change in gut morphology take place between 2 and 4 hours after puparium formation. A layer of adult midgut cells surrounding the remaining larval cells can be distinguished by 6h after puparium formation. Within the next 6h the adult tissue keeps growing, while the larval midgut tissue condenses to the so-called yellow body. (Jiang, et al., 1997)

Stage	Hours[a]	Developmental event (at 25°C)
P1	0–1	White puparium: wriggling stops completely
P2	1–3	Brown puparium: oral armature stops moving permanently, heart stops pumping, gas bubble becomes visible within abdomen
P3	3–6.5	Bubble prepupa: puparium becomes separated from underlying epidermis; bubble in abdominal region is large, causing prepupa to become positively buoyant at end of this stage (it floats)
P4	6.5–12.5	Buoyant and moving bubble: prepupa is buoyant, and bubble moves, first appearing in the posterior of the puparium, displacing pupa anteriorly, and then appearing in the anterior, displacing the pupa posteriorly. Imaginal head sac is everted and oral armature of larva is expelled
P5	12.5–25	Malpighian tubules migrating and white: legs and wings extend; Malpighian tubules move from thorax to abdomen and become visible as white structures in dorsal anterior abdomen
P6	25–43	Green Malpighian tubules: Malpighian tubules turn green, and dark green "yellow body" appears between the anterior ends of the two Malpighian tubules
P7	43–47	"Yellow body": "yellow body" (actually dark green) moves back between the Malpighian tubules; transparent pupal cuticle separates from underlying epidermis; eye cup becomes yellow at its perimeter
P8	47–57	Yellow-eyed: eyes become bright yellow
P9	57–69	Amber: eyes darken to deep amber
P10	69–73	Red-eye Bald: eyes become bright red; orbital and ocellar bristles and vibrissae darken
P11	73–78	Head and thoracic bristles: head bristles, followed by thoracic bristles, darken
P12	73–78	Wings grey: wings become gray; sex comb darkens
P13	78–87	Wings black: wings become black; tarsal bristles darken and claws become black
P14	87–90	Mature bristles: green patch (the meconium–waste products of pupal metabolism) appears dorsally at posterior tip of abdomen
P15	90–103	Meconium and eclosion: tergites become tan, obscuring Malpighian tubules and "yellow body"; legs twitch; flies able to walk prematurely if puparium removed; eclosion completed

Figure 2: Stages of metamorphosis (Tyler, 2000)

Prepupa: P1 (number 7-9), P2 (number 10-13), P3 (number 14,15), P4 (number 16-21) (Bainbridge & Bownes, 1981)

Phanerocephalic pupa: P5 (number 22-26), P6 (number 27), P7 (number 28,29), P8 (number 30-32), P9 (number 33,34), P10 (number 35,36), P11 (number 37,38), P12 (number 39-42), P13 (number 43), P14 (number 44), P15 (number 45-48) (Bainbridge & Bownes, 1981)
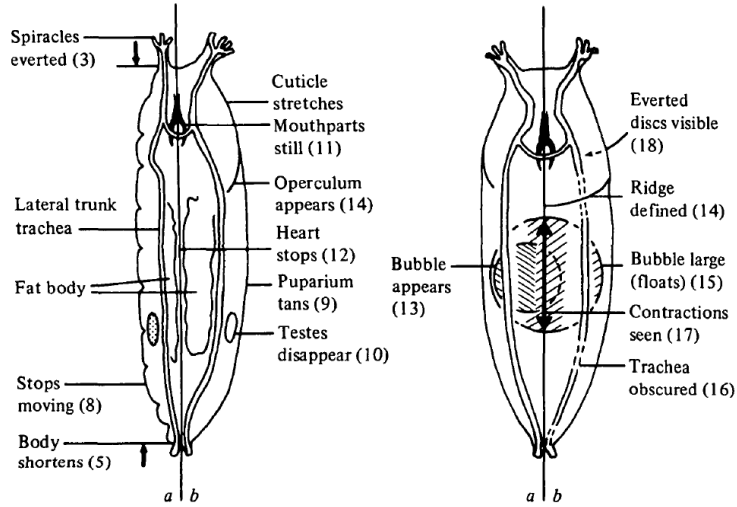
Figure 3: From left to right – stages L1 (post-feeding) to P4 (Buoyant) (Bainbridge & Bownes, 1981)
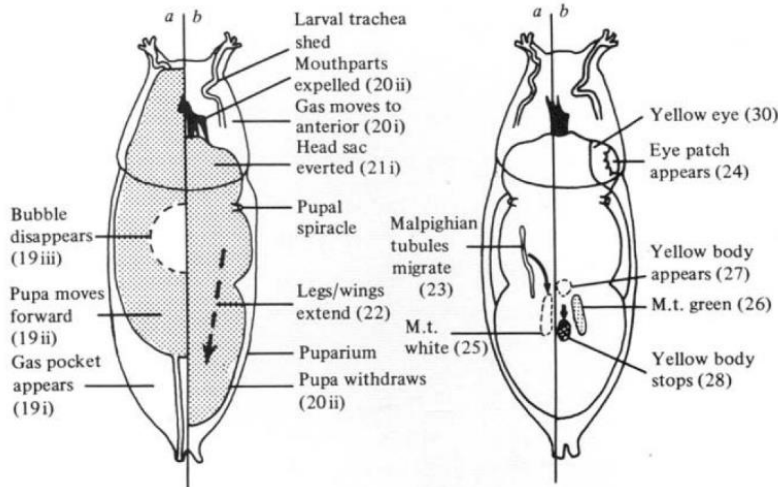

Figure 4: from left to right – stages P4 (moving bubble) to P7(yellow body) (Bainbridge & Bownes, 1981)
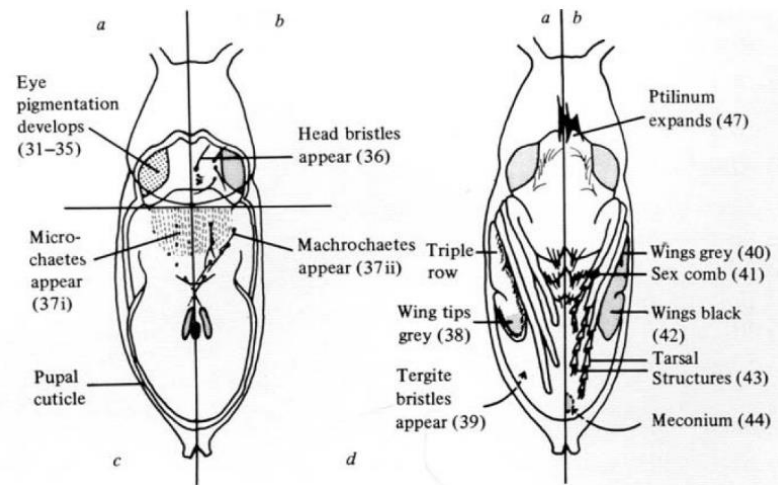

Figure 5: from left to right – stages P8 (yellow-eyed) to P15 (eclosion) (Bainbridge & Bownes, 1981)

Immunology of *Drosophila melanogaster*

Insects like *Drosophila melanogaster* use an innate immune system for defense against infectious pathogens. An Innate immune system is a primary defense response evolutionary conserved among metazoans. Insects possess multiple mechanisms to fight microbial pathogens. Upon infection or wounding proteolytic cascades are stimulated within the insect which lead to blood clotting and the activation of a prophenoloxidase cascade causing melanization. In cellular immunity hemocytes cause phagocytosis, nodulation and encapsulation of pathogens. Antimicrobial peptides (AMP) are produced to fight against systemic as well as local infections. (Flatt, et al., 2008)

Microbial pattern recognition receptors (PRRs), for example peptidoglycan recognition proteins (PGRPs) and Gram-negative binding proteins (GNBPs), recognize pathogens. Pathogen-derived molecules bind to the PRRs which activates both the Toll pathway as well as the immune deficiency (IMD) pathway, immune responses covering Gram-positive and Gram-negative bacteria and fungal pathogens. The Toll pathway activates the nuclear factor kappa B (NF-KB) transcription factors Dorsal and Dif (Dorsal-related immunity factor) which induce AMP gene expression. NF-KB factors initiate transcription of Attacin, Cecropin and Diptericin, which are active against Gram-negative and Gram-positive bacteria, and Drosomycin and Metchnikowin, which are active against fungi. (Flatt, et al., 2008)

In insects the regulation of immune responses through hormones is not fully understood yet. The steroid hormone 20E, an important factor for regulating development, metamorphosis, reproduction and aging, is suggested to play an important role in regulating innate immunity as well. Depending on the developmental stage and the activity of the immune system, 20E can either induce or suppress innate immunity. (Flatt, et al., 2008)

Antimicrobial Peptides

Both systemic and local infections in the insects' body trigger an Antimicrobial peptides (AMP) response. In case of a systemic infection the fat body (the insect equivalent to a liver) produces AMPs and releases them into the hemolymph (the equivalent to a bloodstream). The transcription of AMP genes is initiated by molecular events. (Flatt, et al., 2008)

In this thesis the following AMP genes have been used to represent immune responses during metamorphosis.

Attacin-A (FlyBase, 2020)
Attacin-A (AttA) is a protein coding gene for an antibacterial peptide. This AMP is active against Gram-negative bacteria. Att-A expression takes place in the fat body and several epithelia and is regulated by immune deficiency and, to a lesser extent, Toll pathways.
The Att-A Sequence is located on the chromosome 2R in position 14,747,362 to 14,748,215 on the plus strand. The sequence and further information can be found on Flybase (CG10146, FBgn0012042) or NCBI (GeneID: 36636).
Att-A belongs to the attacin/sarcotoxin-2 protein family. Attacins are small, glycine-rich AMPs. Att-A is involved in the defense against Gram-negative as part of humoral immune response. It also responds to hyperoxia. Mutations of Att-A can lead to partial lethality with some flies dying during pupal stage, immune response defects or oxidative stress response defects. The protein is active in the hemolymph. Figures 6-8 show when and where Att-A is naturally expressed.
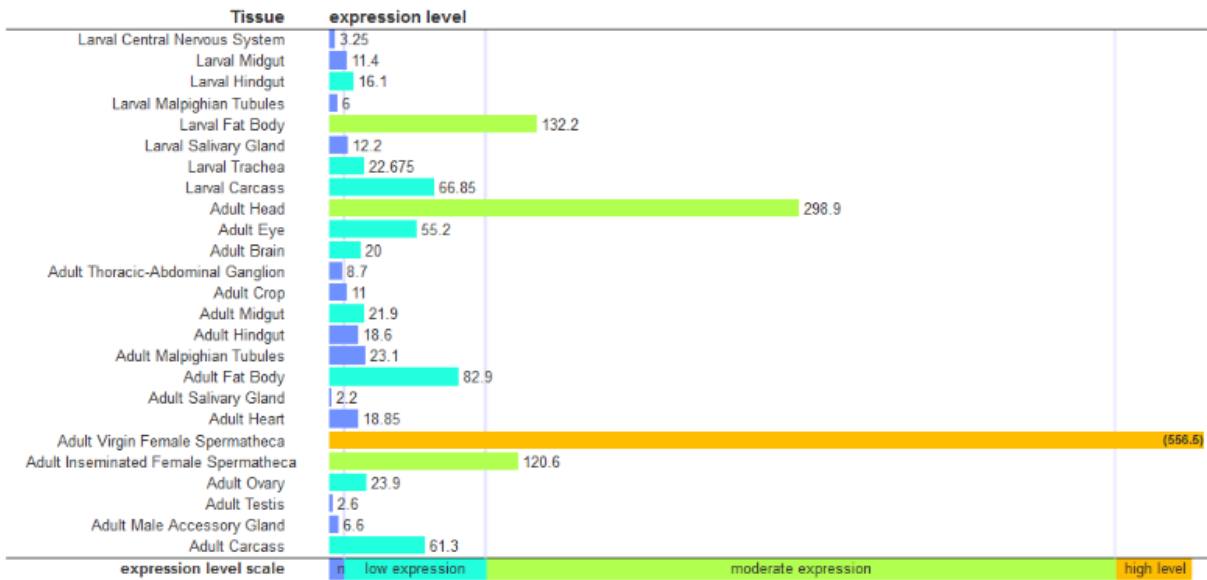
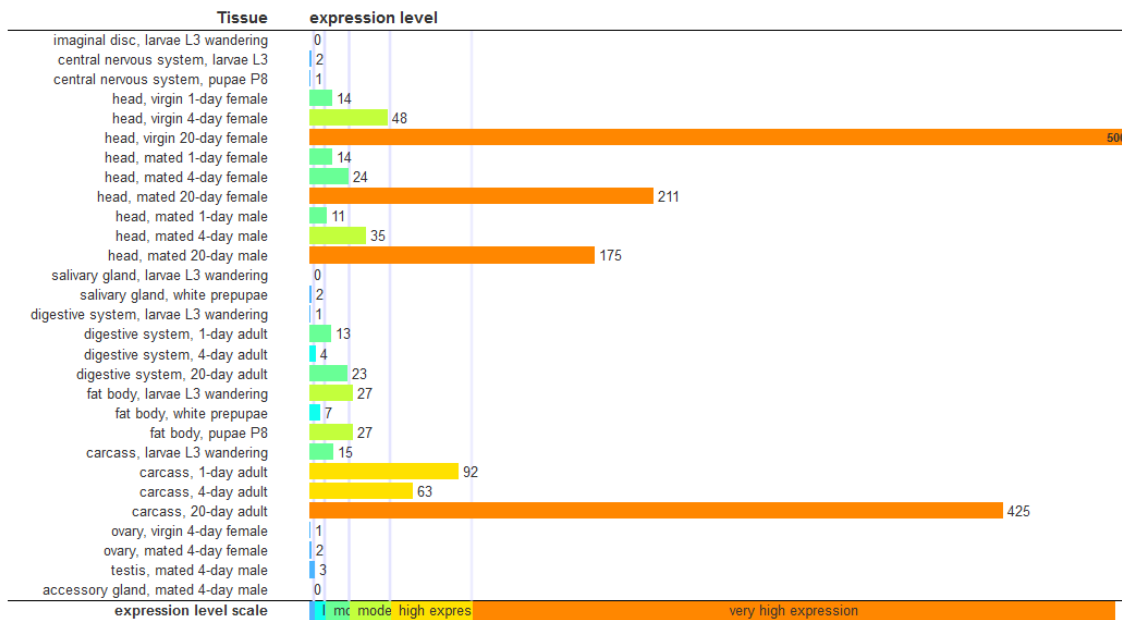*Figure 6: Anatomical Expression of Att-A (FlyBase, 2020)*

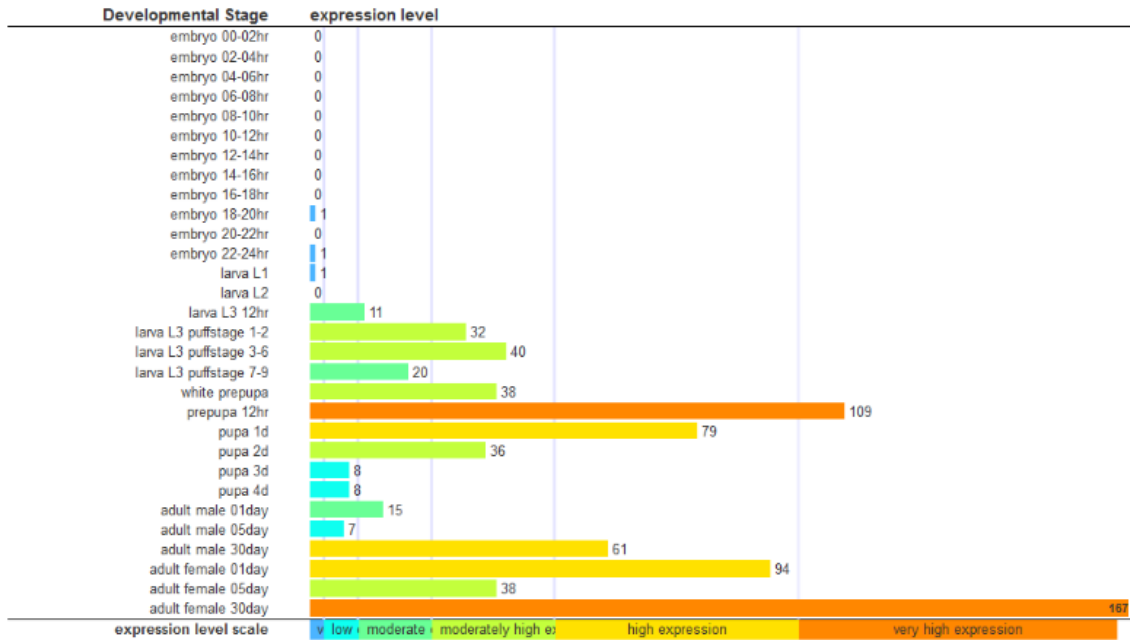*Figure 7: tissue expression of Att-A (FlyBase, 2020)*

Figure 8: Temporal Expression of Att-A (FlyBase, 2020)

Attacin-D (FlyBase, 2020)

Attacin-D is a protein coding gene for AMP against Gram-negative bacteria.

The Att-D sequence is located on the chromosome 3R in position 17,625,268 to 17,626,086 on the plus strand. The sequence and further information can be found on Flybase (CG7629, FBgn0038530) or NCBI (Gene ID: 42122).

Att-D is part of the immune response triggered by stimuli and is involved in the humoral response to Gram-negative bacteria and the response to hyperoxia. Mutations in Att-D lead to exocytosis defects. When and where Att-D is naturally expressed can be seen in figures 9-11.
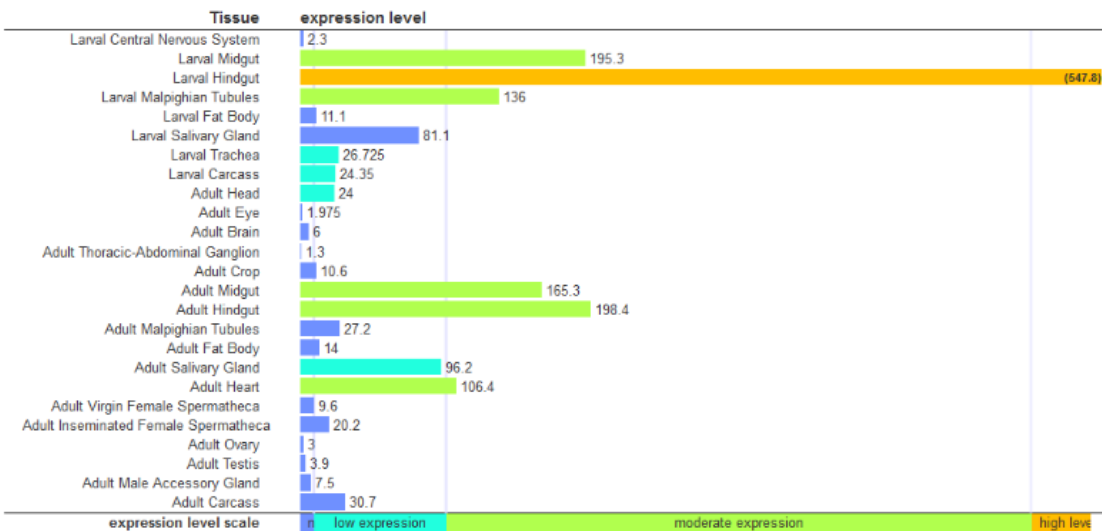
Figure 9: Anatomical expression of Att-D (FlyBase, 2020)
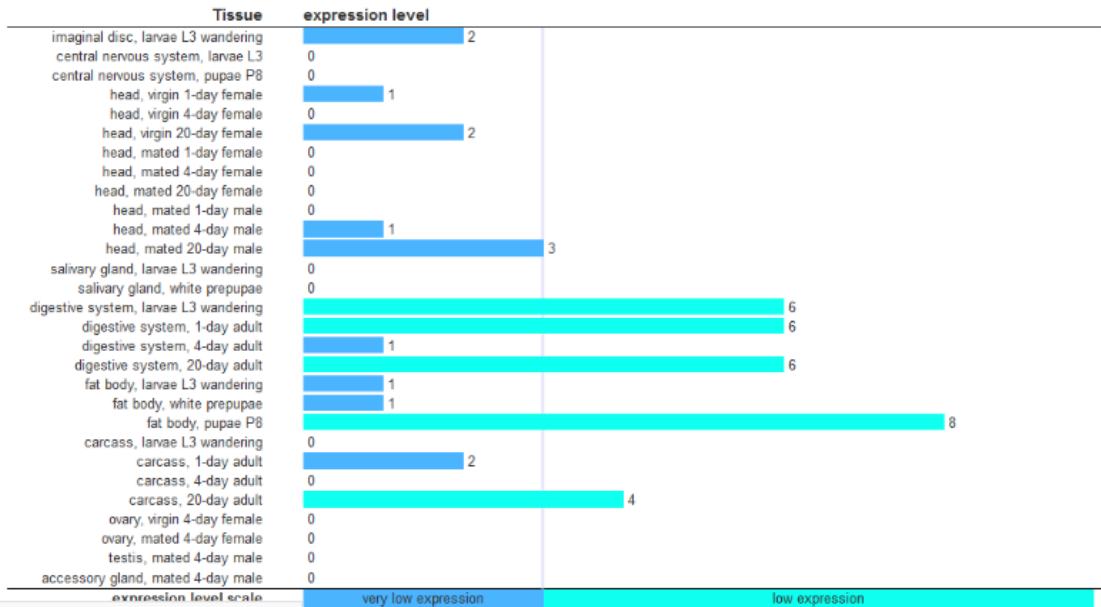
Figure 10: Tissue expression of Att-D (FlyBase, 2020)
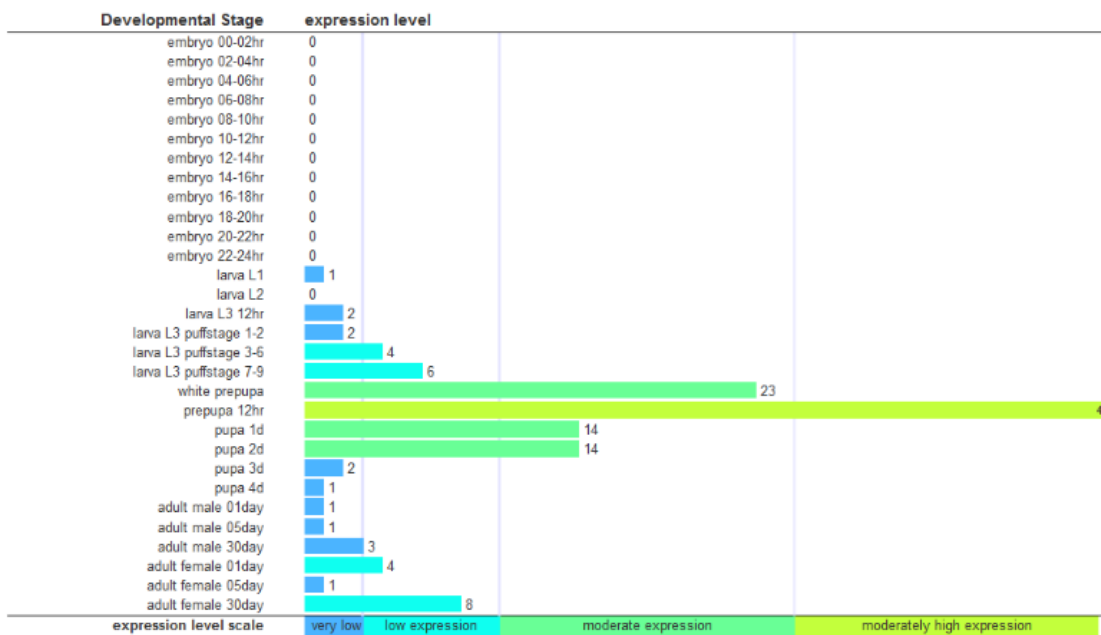
Figure 11: Temporal Expression of Att-D (FlyBase, 2020)

Cecropin A1 (FlyBase, 2020)

Cecropin A1 (CecA1) is a protein coding gene for an AMP active against Gram-negative bacteria which is expressed in the fat body upon the systemic immune response and in several epithelia. Its transcription is mainly regulated by the immune deficiency pathway.

The location of the CecA sequence is the chromosome 3R in position 30,210,874 to 30,211,273. The sequence and further information can be found on Flybase (CG1365, FBgn0000276) or NCBI (Gene ID: 43596).

CecA is involved in antibacterial humoral response against Gram-negative bacteria. Mutations lead to body color defects. CecA1 is one of three Cecropin proteins, cecropin A1, A2, and B. In figures 12 and 13 the location and time of natural expression can be seen.
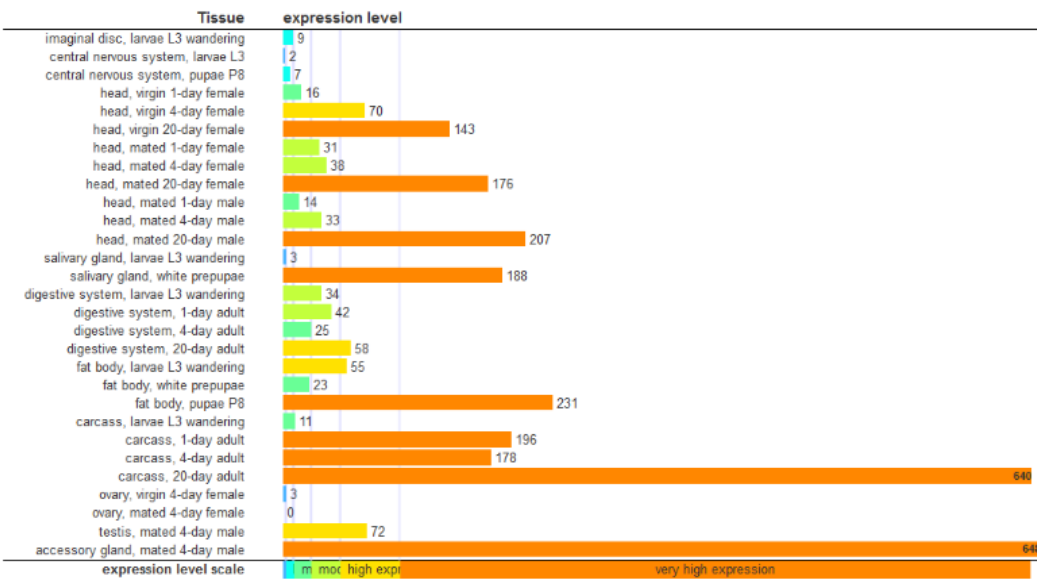
Figure 12: CecA tissue expression (FlyBase, 2020)
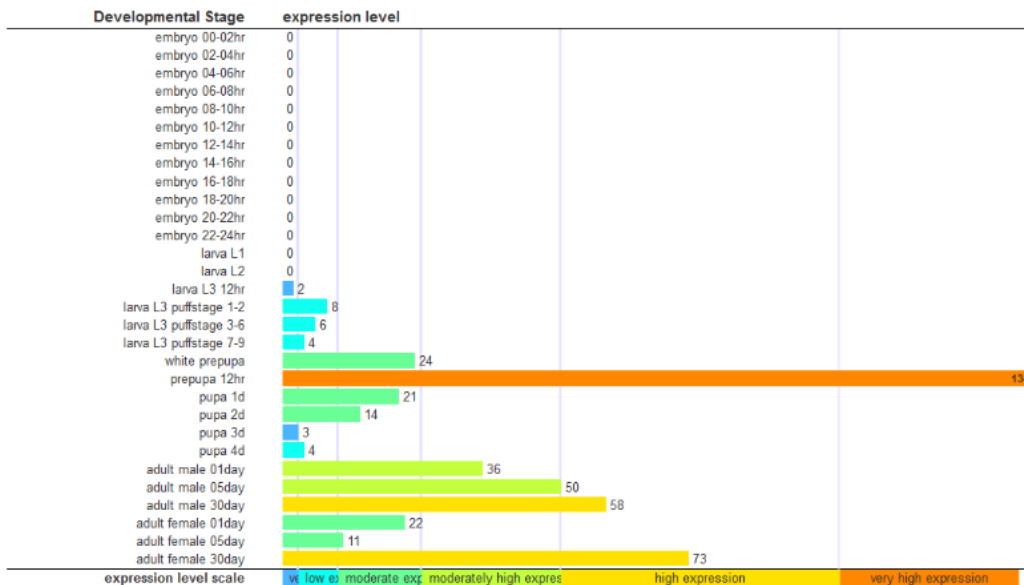
Figure 13: CecA temporal expression (FlyBase, 2020)

Defensin (FlyBase, 2020)

Defensin (Def) in a protein coding gene for an AMP active against Gram-positive bacteria. Def is induced in the fat body in the course of systemic immune response and is expressed in several epithelia. The transcription of Def is dependent on both the immune deficiency and the Toll pathways.

The Def sequence is located in the chromosome 2R in the position 10,054,178 to 10,054,576. The sequence and further information can be found on Flybase (CG1385, FBgn0010385) or NCBI (Gene ID: 36047).

Def belongs to the invertebrate defensin protein family. This AMP is involved in antibacterial humoral active against Gram-positive bacterium. Mutations of Def affect the adult brain and can lead to shorter lifespan, neuroanatomy defects and immune response defects. Def is acting in the hemolymph and also shows expression in the absence of immune challenge during metamorphosis. It is found in the circulary, adipose and reproductive system. Figure 14-16 show the location and timepoint of Def expression.

Figure 14: Def Anatomical expression (FlyBase, 2020)
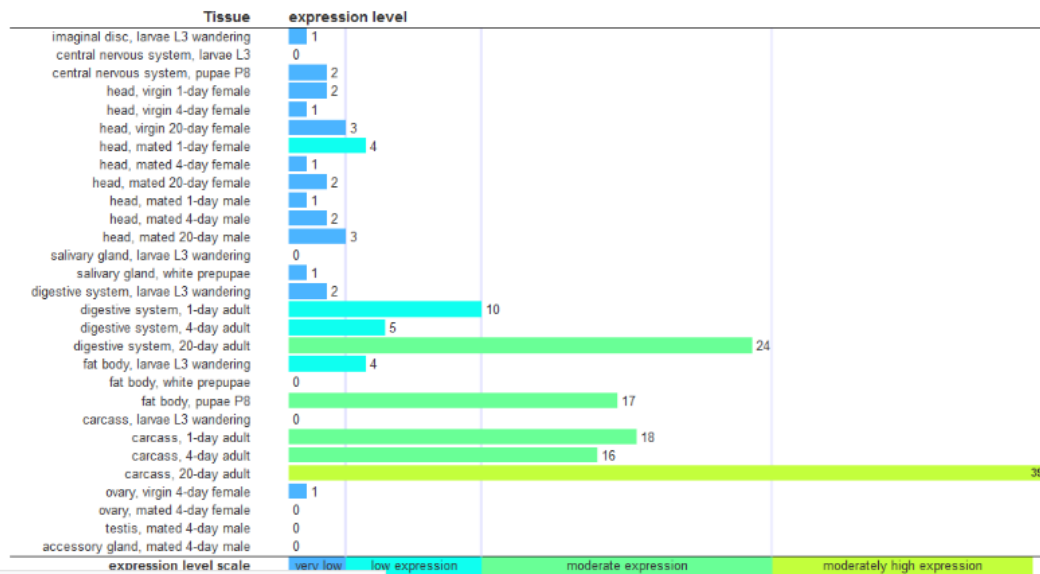
Figure 15: Def tissue expression (FlyBase, 2020)
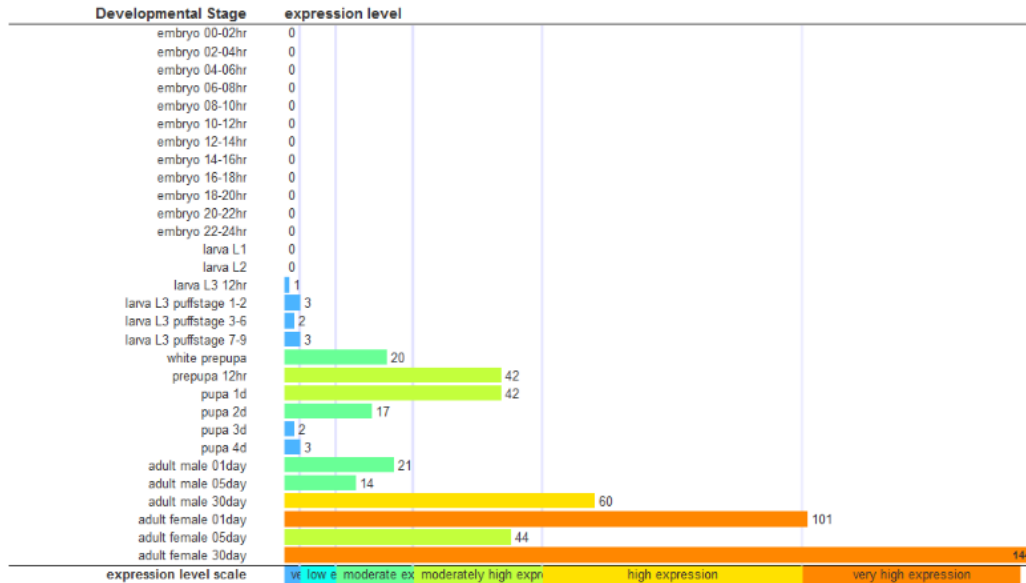
Figure 16: Def temporal expression (FlyBase, 2020)

Diptericin A (FlyBase, 2020)

Diptericin A (DptA) encodes an AMP induced upon immune challenge with activity against Gram-negative bacteria. During the systemic immune response DptA is expressed in the fat body and in several epithelia. Regulation of DptA transcription happens via the immune deficiency pathway.

The DptA sequence is located on the 2R chromosome in position 18,865,765 to 18,866,260. The sequence and further information can be found on Flybase (CG12763, FBgn0004240) or NCBI (Gene ID: 37183).

DptA belongs to the attacin/sarcotoxin-2 family and is involved in anti-Gram-negative bacterial humoral response and response to hyperoxia. Mutations of DptA manifest in mesothoracic tergum and the adult posterior midgut epithelium and can lead to lethality during pupal stage, oxidative stress response defects. Figure 17-19 show the expression levels of DptA in regard to location and developmental stage.
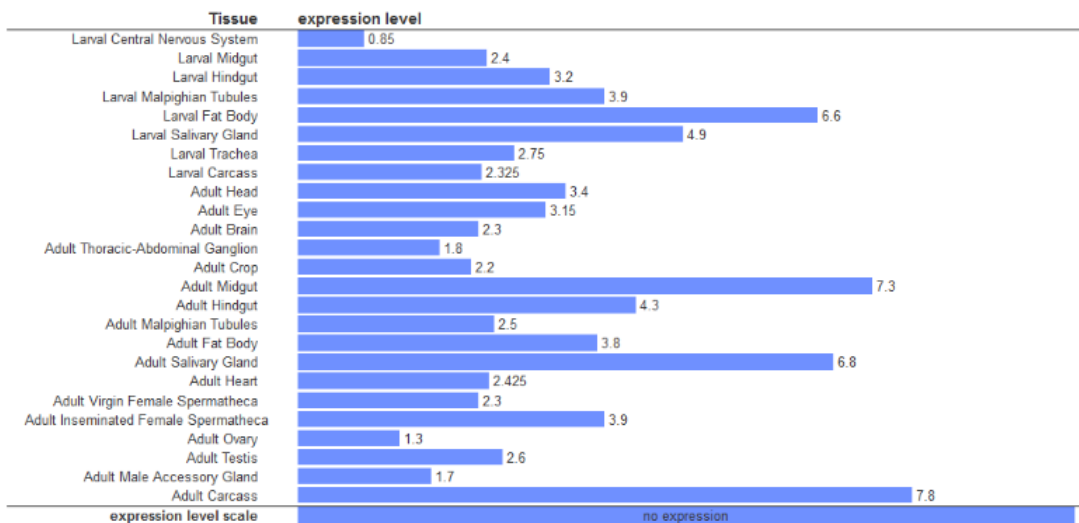
Figure 17: DptA Anatomical expression (FlyBase, 2020)
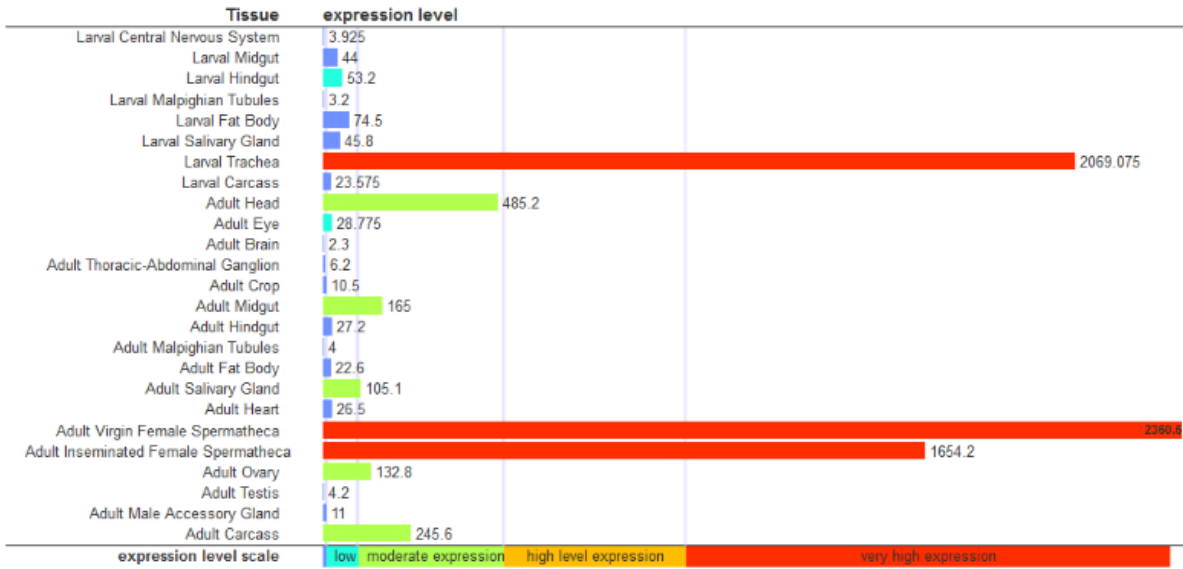
Figure 18: DptA Tissue expression (FlyBase, 2020)

Figure 19: DptA temporal expression (FlyBase, 2020)

Metchnikowin (FlyBase, 2020)

Metchnikowin (Mtk) is the protein coding gene for an antifungal peptide produced in and released from the fat body during the systemic immune response and is also synthesized by several epithelia. MTK transcription is regulated by the immune deficiency and/or Toll pathways.
The MTK sequence is located on the chromosome 2R in position 15,408,846 to 15,409,113. The sequence and further information can be found on Flybase (CG8175, FBgn0014865) or NCBI (Gene ID: 36708).

MTK is active as a potent antifungal peptide and AMP against Gram-positive bacteria. Figures 20-22 show expression levels of MTK in regard to location and timepoint.
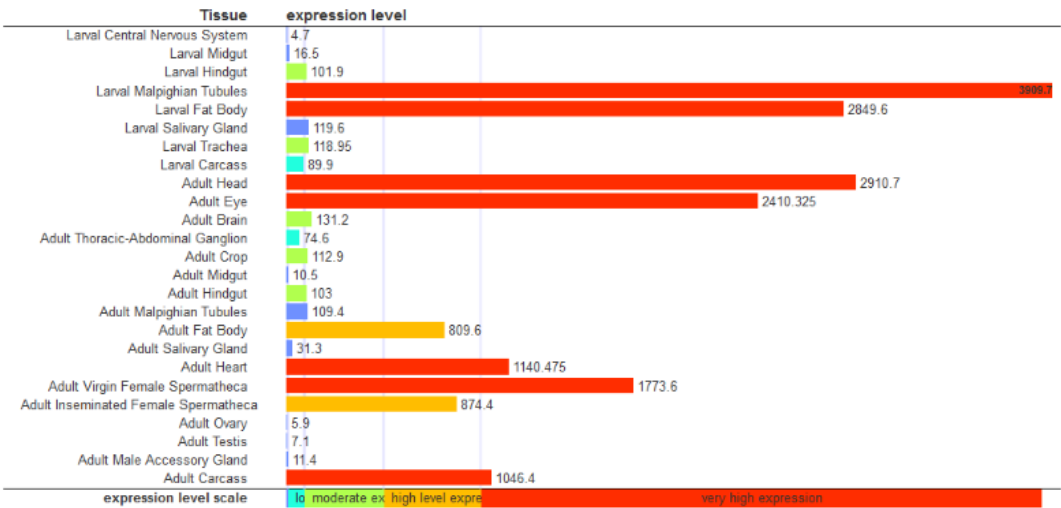
Figure 20: MTK Anatomical expression (FlyBase, 2020)
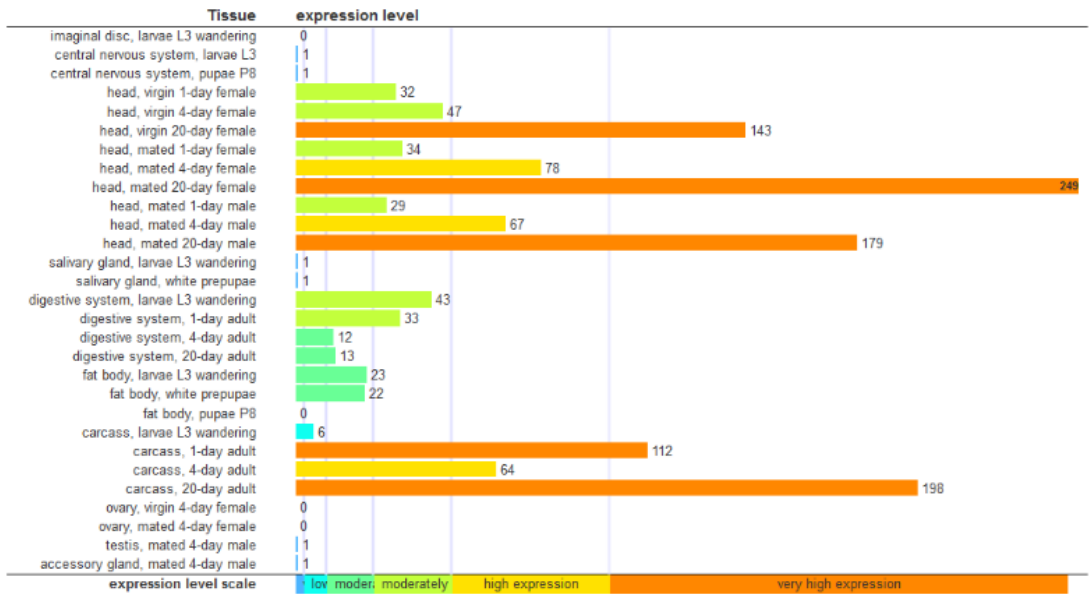
Figure 21: MTK Tissue expression (FlyBase, 2020)
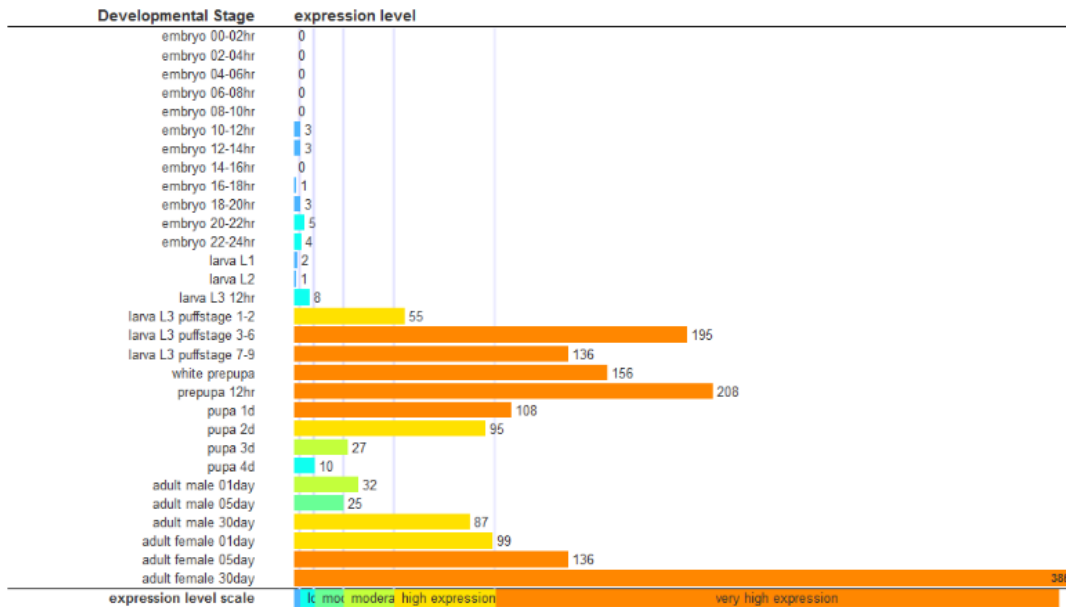
Figure 22: MTK Temporal expression (FlyBase, 2020)

Drosocin (FlyBase, 2020)

Drosocin (Dro) encodes an o-Glycosylated AMP for defense against Gram-negative and Gram-positive bacteria. As the other AMPs, Dro is expressed in the fat body during systemic immune response and is also expressed in several epithelia. The immune deficiency pathway regulates Dro transcription.

The Dro sequence is located on the chromosome 2R in position 14,745,961 to 14,746,714. The sequence and further information can be found on Flybase (CG10816, FBgn0010388) or NCBI (Gene ID: 36635).

The AMP Dro belongs to the Drosocin protein family. Mutations affect the adult brain which can lead to neuroanatomy defects. Figures 23-25 show tissue- and stage-specific expression levels of Dro.

Figure 23: Dro Anatomical expression (FlyBase, 2020)

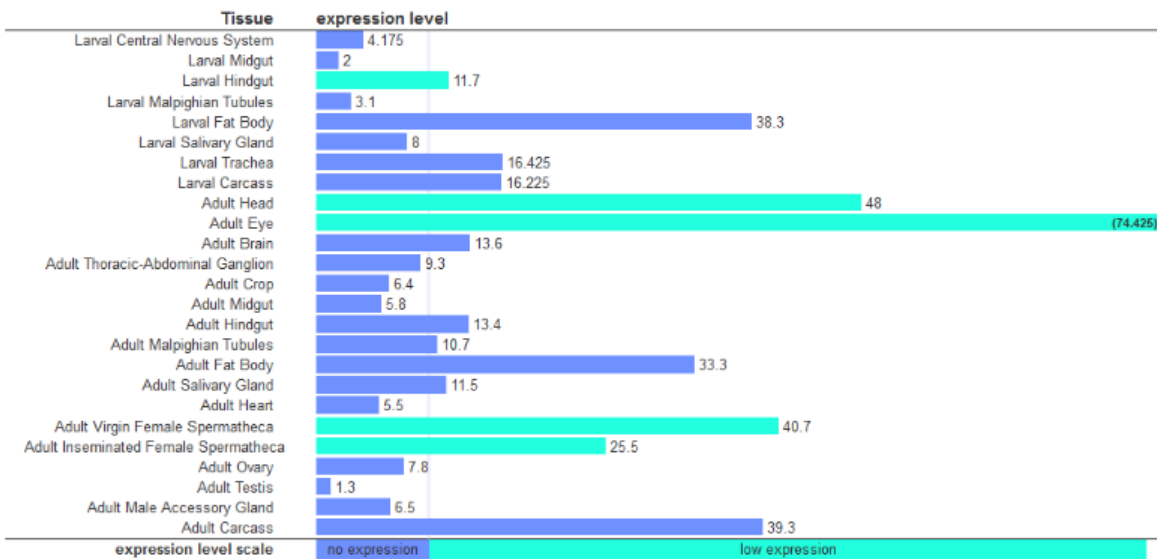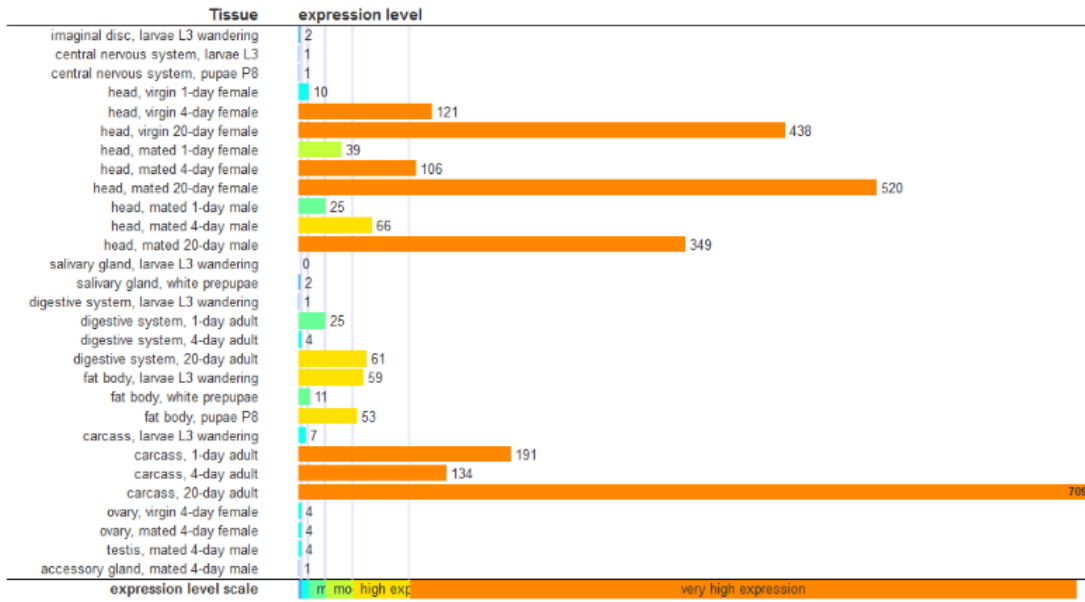| Tissue	expression level
imaginal disc, larvae L3 wandering	2
central nervous system, larvae L3	1
central nervous system, pupae P8	1
head, virgin 1-day female	10
head, virgin 4-day female	121
head, virgin 20-day female	438
head, mated 1-day female	39
head, mated 4-day female	106
head, mated 20-day female	520
head, mated 1-day male	25
head, mated 4-day male	66
head, mated 20-day male	349
salivary gland, larvae L3 wandering	0
salivary gland, white prepupae	2
digestive system, larvae L3 wandering	1
digestive system, 1-day adult	25
digestive system, 4-day adult	4
digestive system, 20-day adult	61
fat body, larvae L3 wandering	59
fat body, white prepupae	11
fat body, pupae P8	53
carcass, larvae L3 wandering	7
carcass, 1-day adult	191
carcass, 4-day adult	134
carcass, 20-day adult	709
ovary, virgin 4-day female	4
ovary, mated 4-day female	4
testis, mated 4-day male	4
accessory gland, mated 4-day male	1
expression level scale	m mo high exp very high expression

Figure 24: Dro tissue expression (FlyBase, 2020)

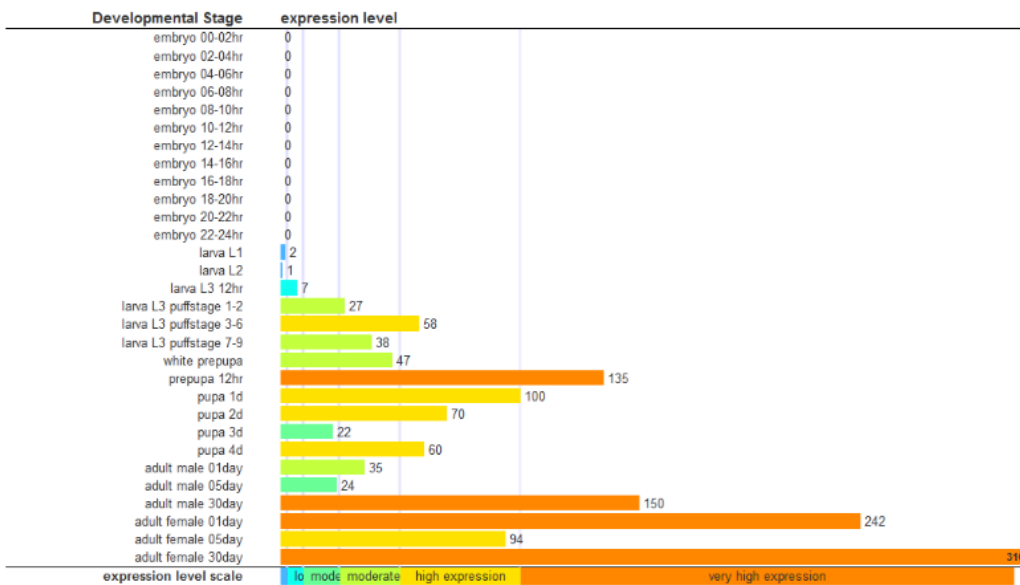| Developmental Stage	expression level
embryo 00-02hr	0
embryo 02-04hr	0
embryo 04-06hr	0
embryo 06-08hr	0
embryo 08-10hr	0
embryo 10-12hr	0
embryo 12-14hr	0
embryo 14-16hr	0
embryo 16-18hr	0
embryo 18-20hr	0
embryo 20-22hr	0
embryo 22-24hr	0
larva L1	2
larva L2	1
larva L3 12hr	7
larva L3 puffstage 1-2	27
larva L3 puffstage 3-6	58
larva L3 puffstage 7-9	38
white prepupa	47
prepupa 12hr	135
pupa 1d	100
pupa 2d	70
pupa 3d	22
pupa 4d	60
adult male 01day	35
adult male 05day	24
adult male 30day	150
adult female 01day	242
adult female 05day	94
adult female 30day	310
expression level scale	lo mode moderate high expression very high expression

Figure 25: Dro temporal expression (FlyBase, 2020)

Juvenile Hormone

Role of Juvenile hormone (JH)

Juvenile hormones belong to the important sesquiterpenoid hormones. The class of sesquiterpenoid hormones can be found in all Artropods with juvenile hormones being present

Figure 26: Structure of JH (Tamone, 1997)

in insects as the natural occurring hormone JH III (methyl epoxy farnesoate). The structure of methyl epoxy farnesoate can be seen in figure 26. (Jindra, et al., 2015)
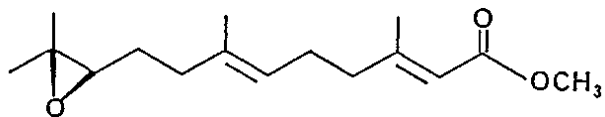
JH is an endocrine signal, which is released into the hemolymph after production in the gland known as corpus allatum (CA). In Drosophila larvae, the CA is an integral part of the ring gland in which the synthesis of the steroid hormone ecdysone takes place as well. (Flatt, et al., 2008) (Schwenke & Lazzaro, 2017)

JH regulates insects' development by influencing metamorphosis, growth, aging and lifespan, polymorphism and determines the social caste. (Jindra, et al., 2015) (Schwenke & Lazzaro, 2017) (Flatt, et al., 2008) JH facilitates reproduction while it acts as an immune suppressor. (Schwenke & Lazzaro, 2017) JH III was found to significantly suppress the basal expression of multiple AMPs. (Jindra, et al., 2015) JH downregulates the transcription of immune response genes with or without an infection being active. JH may function as molecular trigger to invest more energy and resources into reproduction than into immunity. (Schwenke & Lazzaro, 2017) JH also regulates expression of AMPs that are not part of the immune response. It was found to induce the expression of the Ceratotoxin A, a specific AMP not expressed in response to infection. (Flatt, et al., 2008)Removing the CA leads to reduced JH synthesis and therefore reduced immune suppression. JH may act to downregulate the immune system to prevent autoimmunity. (Schwenke & Lazzaro, 2017)

Artificial JH

Methoprene and pyriproxyfen (PRX) are substances with the same effect as the natural hormone JH III and are synthetic JH analogs (JHa). (Jindra, et al., 2015) (Schwenke & Lazzaro, 2017)Pyriproxyfen is a potent JH mimic which has a distinct, pyridine-based structure. JHa are chemically and biologically more stable than naturally occurring JH III which explains their higher potency to activate JH-responsive elements. (Jindra, et al., 2015) The inhibiting effects on immunity of JH III could be observed for JHa methoprene and pyriproxyfen as well. Both JH and JHa suppress the genes required for innate immune responses, including multiple AMP genes. (Jindra, et al., 2015) (Schwenke & Lazzaro, 2017) 10^{-2}µg methoprene applied were found to block immune system activation by suppressing the induction of AMPs. (Schwenke & Lazzaro, 2017)Because of the role JH plays in the development of insects, JH mimicking compounds like methoprene are also used as insecticides. (Jindra, et al., 2015)

Methoprene and pyriproxyfen all compete with JH III for binding to the receptor protein Gce, and therefore function as true agonists to JH III. (Jindra, et al., 2015)

Relationship with 20-Hydroxy-ecdysone

JH is believed to regulate immune responses in cooperation with the steroid hormone 20-Hydroxy-ecdysone (20E). Both hormones play an important role in the regulation of gene expression in response to immune challenges. 20E was suggested to be a positive regulator of innate immunity, while JH has an immune suppressing effect. 20E was found to promote humoral immunity by enhancing AMP expression with JH specifically and strongly inhibiting this effect. 20E is required for efficient AMP transcription upon immune challenge with JH then suppressing the response. JH is an 20E antagonist which possesses immune suppressing qualities on its own but has a bigger immune suppressive effect when the immune response is prior enhanced by 20E. JH has the ability to rapidly and specifically counteract increased immune responses from 20E but is not interfering with any other cellular processes dependent on 20E. (Flatt, et al., 2008)

JH and 20E both target several tissues including brain, gonads, fat body and endocrine tissue. The main production site of AMPs is in the fat body after systemic infection, so it is reasonable to assume the immune regulation by 20E and JH takes place in this tissue as well. (Flatt, et al., 2008)

The ecdysone signaling pathway includes the nuclear hormone receptors EcR and UsP. The activation of AMPs by 20E is via the EcR/USP heterodimer, which may also be required for AMP suppression by JH. (Flatt, et al., 2008)

JH function

JH is hydrophobic and needs a carrier to be transported in the bloodstream. Without the carrier to keep it soluble and protected it would be degraded by breaking the ester bond. The carrier transports the JH molecules to the cell membrane where the change in pH causes the JH to be released. Met and Gce, which are first bound to a chaperone molecule then bind to JH and transport it into the nucleus. In the nucleus *gce*, *Met* and JH form a complex with *tai* which can then bind DNA. This complex functions as a transcription factor that activates transcription. The simplified process is depicted in figure 27.
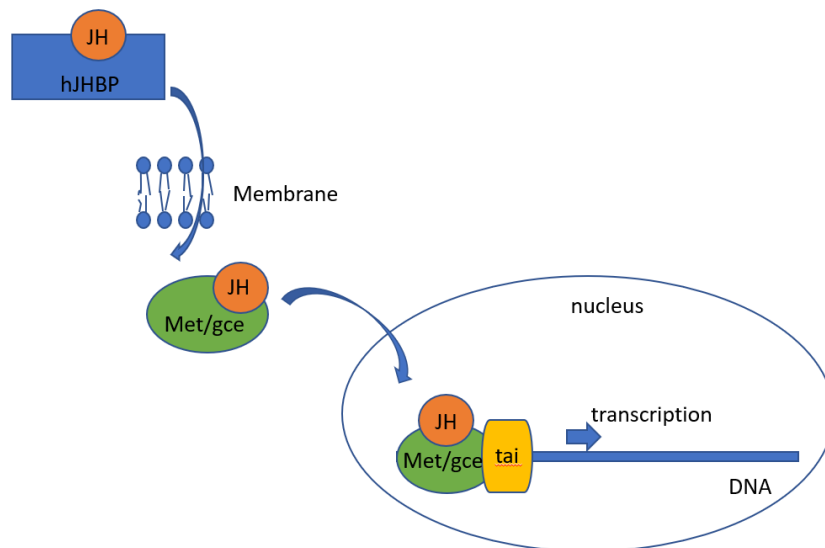

Figure 27: JH function

Juvenile Hormone Receptors

Met and Gce

In *Drosophila melanogaster* Methoprene-tolerant (Met) and germ cell expressed (Gce) are paralogs that arose by gene duplication during the "higher fly" evolution. The genes encoding both Gce and Met proteins lie on the X chromosome. Most other insect species only possess the Met gene for the function of gce/Met. *Drosophila melanogaster* Gce is more similar to the Met gene of other insect species, which correlates with the finding that *Drosophila* Gce is the ancestral gene to *Drosophila* Met. (Jindra, et al., 2015)

Met and gce are both part of the basic helix-loop-helix (bHLH)/Per-Arnt-Sim (PAS) transcription factor family. Met and Gce are JH receptors and play an essential role in insect development by mediating JH signalling. (Jindra, et al., 2015) (Schwenke & Lazzaro, 2017)During development the paralogs appear to

have the same function, making the presence of both redundant, but in other JH-dependent biological processes their functionality differs. (Schwenke & Lazzaro, 2017)

In the process of immune suppression dependent on JH, activation of transcription in response to JH signals is mediated by Gce. Fully functional gce is needed for a functional JH response, while only a complete lack or loss of function mutation of Met prevents JH signalling. In the presence of wildtype Gce, immune suppression is independent from Met. Therefore, regarding immunity, Gce has the dominant mediating effect although functional Gce and Met are mutual substitutes. (Jindra, et al., 2015)

JH mimicking insecticides kill *D. melanogaster* with both functional Met and Gce present. Genotypes with mutated Met gene show resistance to these insecticides. Mutants with unfunctional Gce show resistance as well, but to a lesser extent. (Jindra, et al., 2015)

Met and Gce interact with the chaperone Hsp83, which facilitates import of Met into the nucleus and JH induced gene expression. MF, the precursor of JH, acts as a hormone itself and mediates its effects through Gce and Met. (Jindra, et al., 2015)

Met and Gce have a high affinity to JH. Mutations in the PAS-B domain of Met inhibit JH binding. In *D. melanogaster* Met, the residues T406, V449 and C500 are crucial for a functional binding site. (Jindra, et al., 2015)

Like Met, Gce was found to bind natural *Drosophila melanogaster* JH III, methyl farnesoate, and JH analogs and mediates the hormone's essential role during development of the fruit fly. JH III is an activating ligand for Gce. In the Gce binding site three amino acids, T272, V315 and C366, are crucial for correct JH binding. Comparison with the corresponding residues in Met genes of other insects has led to the assumption that these positions are conserved among species. Correct binding of JH to Gce is necessary for transcription to be induced. (Jindra, et al., 2015) The suppression of immunity in *D. melanogaster* in favor of reproduction is mediated through the Gce receptor. (Schwenke & Lazzaro, 2017)

The JH binding event causes Met to bind another bHLH-PAS protein called Taiman (Tai), as can be seen in figure 3. The resulting complex is able to bind specific DNA motifs responding to JH signals and activate the targeted gene transcription of these DNA motifs. Like Met, Tai was found to function as mediator of JH-dependent processes in metamorphosis and reproduction. Tai and Gce are necessary for functional JH response during immune challenge. (Jindra, et al., 2015)

Double mutation of Gce and Met
In *D. melanogaster*, mutation of Met and deletion of its paralog Gce causes 100% lethality during larva-pupa transition. This effect corresponds to the crucial phase in which lack of JH results in death of *D. melanogaster*. $gce^{2,5k}$ and Met^{27} are both loss of function alleles. In the $gce^{2,5k}$ Met^{27} double mutant the expression of kr-h1, a direct target of Gce/Met mediated JH response, is lowered. Kr-h1 is essential for *D. melanogaster* to complete the prepupal stage. Reduced kr-h1 expression in double mutants may contribute to the lethality rate in this stage. (Jindra, et al., 2015)

Transfection of either fully functional Met or Gce can restore JH dependent functions like kr-h1 expression and recover viability of flies lacking both endogenous Met and Gce. (Jindra, et al., 2015)

Aim of the thesis

JH influences *Drosophila melanogaster* development and is also affecting the immune system. In this thesis we hypothesize that the histolysis of tissue and extensive remodelling of the flies' body lead to an immune challenge during metamorphosis. The role of JH during metamorphosis could therefore be both developmental and immune regulating.

Expression of AMPs during metamorphosis is altered, perhaps through JH-dependent regulation, but whether AMPs are solely part of immunity or also play a developmental role in the pupal stage is still unknown. Also, the part played by the JH receptor genes Gce and Met is in question.

For this thesis, experiments have been designed to show the impact of the presence or absence of JH and its receptors on the immune response represented by AMP mRNA expression during metamorphosis. Anticipated results could show the role JH and its receptors play in immune regulation during development of *Drosophila melanogaster*.

Methods

Experimental assembly

For investigating the effect of JH on *Drosophila melanogaster* during metamorphosis 3 different approaches were taken. In preliminary experiments all materials and methods were tested before applying them to the real samples. 3 different genotypes were used, 1 wildtype-like as control and 2 mutated genotypes with unfunctional JH receptors and therefore disrupted JH effect.

For investigating which AMPs are expressed during the events of metamorphosis, pupae of known age were collected and, after RNA isolation and cDNA synthesis, q-RT-PCR gave the amount of AMPs expression at this stage, resulting in a profile of AMP expression over a course of 72 hours.

For investigating the effect of JH directly, pupae of a known age were treated with PRX, a JHa. After RNA isolation and cDNA synthesis, q-RT-PCR gave the amount of AMPs expressed in this setting.

Lastly flies were crossbred to obtain *Drosophila melanogaster* genotypes with AMPs that were labeled *in vivo*. Larvae of stage 3 were collected and separated into males and females. After pupation they were observed under the microscope at different timepoints to check for signs of the labeled AMPs and possible differences in males and females. Proper detection of the labelled AMPs *in vivo*, locations and timepoints of the AMP observations were investigated.

These experiments could give a more detailed knowledge of the effects JH has on the immune system during metamorphosis.

Drosophila melanogaster genotypes

During these experiments 3 different *Drosophila melanogaster* genotypes were compared.

y w:
yellow: yellow (y) is a protein coding gene. Mutations leading to a lack of y function result in a distinct yellow color of the adult flies' cuticle. (FlyBase, 2020)
white: white (w) is encoding a transporter of the ABCG2 class which transports molecules including pigments like drosopterins and ommochromes. Mutating w results in flies with white eyes. (Flybase, 2020)

This genotype was used for comparison as wildtype-like, since all domains effected by JH are unimpaired.

w Met[27]:
white: white (w) is encoding a transporter of the ABCG2 class, which transports molecules including pigments like drosopterins and ommochromes. Mutating w results in flies with white eyes. (Flybase, 2020)
Met[27]: Met[27] is a loss of function allele of the Met receptor. (FlyBase, 2020)

w gce[2,5k]:
white: white (w) is encoding a transporter of the ABCG2 class, which transports molecules including pigments like drosopterins and ommochromes. Mutating w results in flies with white eyes. (Flybase, 2020)
gce[2,5k]: gce[2,5k] is an amorphic allele of the Gce receptor. A complete lack of function was proven, either by an inactivation of the gene or no gene product at all. (Flybase, 2020)

Samples

All *Drosophila melanogaster* stocks were reared on a standard fly food medium consisting of a mixture of cornmeal, sugar, yeast and agar at 25°C*.* Flies of the genotypes *w gce[2,5k]* and *y w* were transferred to new vials every 2 days, w *Met[27]* every 4 days since the reproduction rate was lower.

Pupae whose metamorphosis were stopped at a chosen timepoint:
For investigating the immune response during development in the pupal stage, pupae from all three genotypes, 2 with mutated JH receptors and 1 control, were collected at chosen timepoints. The white pupa (WP) stage was used as starting point (t=0). WP were marked on the outside of the vial and the exact time and the date noted. The pupae were then collected at the desired timepoint (for example 24h after the prepupae stage), killed by freezing in liquid nitrogen and stored at -80°C. One sample consisted of 3 collected pupae.

Pupae treated with artificial JH:
For investigating the effect of JH directly on pupae during metamorphosis, 6 pupae of each genotype were collected as WP. 3 of them were treated with pyriproxyfen (PRX), a JH analog. PRX is soluble in acetone and can penetrate the pupa and get into the cells because of its hydrophobicity, while the acetone evaporates. The WP were covered in 0,5µl acetone solution containing 200ng pyriproxyfen. The remaining 3 WP were covered in pure acetone as control group. All pupae were then frozen at -80°C 18 hours after their WP stage.

Crossbreeding new genotypes with labelled AMPs:
Crossbreeding should result in flies with labeled AMP genes that simultaneously carry the mutated JH receptor genes. Virgin females of all 3 genotypes were collected and put in a vial with males carrying the genes for AMPs labelled with 2 different markers. GFP is a fluorescent marker and could therefore be observed *in vivo* under UV light, while western blotting was necessary for investigating the lac-Z labelled AMP and quantifying the amount of AMP expression in all genotypes.

Table 1: crosses for genotypes carrying both mutated JH receptor and labeled AMP genes

Female	Male	+; Att-A-GFP	+; Def-GFP	+; CecA1-GFP	+; $\frac{Drosomycin-GFP}{TM3,Sb}$	+; Dpt-lac-Z

y, w	$y\,w\,;\,Att\text{-}A\text{-}GFP$	$y\,w\,;\,Def\text{-}GFP$	$y\,w\,;\,CecA1\text{-}GFP$	$y\,w\,;\,\dfrac{Drosomycin-GFP}{TM3,Sb}$	$y\,w\,;\,Dpt\text{-}lac\text{-}Z$
w, Met^{27}	$w\,Met^{27}\,;\,Att\text{-}A\text{-}GFP$	$w\,Met^{27}\,;\,Def\text{-}GFP$	$w\,Met^{27}\,;\,CecA1\text{-}GFP$	$w\,Met^{27}\,;\,\dfrac{Drosomycin-GFP}{TM3,Sb}$	$w\,Met^{27}\,;\,Dpt\text{-}lac\text{-}Z$
$w, gce^{2,5k}$	$w\,gce^{2,5k}\,;\,Att\text{-}A\text{-}GFP$	$w\,gce^{2,5k}\,;\,Def\text{-}GFP$	$w\,gce^{2,5k}\,;\,CecA1\text{-}GFP$	$w\,gce^{2,5k}\,;\,\dfrac{Drosomycin-GFP}{TM3,Sb}$	$w\,gce^{2,5k}\,;\,Dpt\text{-}lac\text{-}Z$

For *y w* and *w gce^{2,5k}* 5 virgin females and for *w Met^{27}* 10 virgin females were put in a vial with 2-3 males from 1 genotype resulting in 15 crosses that can be seen in table 1.

Larvae of stage 3 of the new genotypes were collected and separated into male and female. After pupation they were collected as WP to know their age.

RNA Isolation

RNA was isolated from pupae tissue using 2 different methods. Below both methods are described in detail and their efficiency and product quality were compared.

RNeasy Plus Micro Kit

This method was used according to the protocol the kit came with.

Procedure:
Before the kit was used the weight of the sample tissue had to be determined to make sure it was below 5mg. Furthermore, 20µl 2M DTT had to be added per 1ml buffer RLT Plus before it could be used. 44ml ethanol were added to the "Working solution" of the kit before the start as well.

1. The tissue (3 frozen pupae) was put in a 1,5ml Eppendorf container and 350µl RLT buffer were added. The tissue was disrupted, and the mixture then centrifuged (3min, maximum velocity).
2. The supernatant from Step 1 was then transferred to the prepared Eliminator Spin column stuck in a 2ml collection tube. Centrifugation (30s, above 8000xg=10 000rpm) followed. The column was then discarded.
3. 350µl 70% ethanol were added to the flow through from Step 2 and mixed by pipetting up and down.
4. The solution was then transferred to the prepared RNeasy MinElute spin column stuck in a 2ml collection tube. Centrifugation (15s, above 8000xg) followed. The flow through was discarded.
5. 700µl RW1 buffer from the kit were added to the column. Centrifugation (15s, above 8000xg) followed. The flow through was discarded.
6. 500µl RPE buffer from the kit were added to the column. Centrifugation (15s, above 8000xg) followed. The flow through was discarded.
7. 500µl 80% ethanol were added to the column. Centrifugation (2min, above 8000xg) followed. The flow through was discarded.
8. The MinElute column was put into a new 2ml collection tube. Centrifugation (5min, full speed) followed. The flow through was discarded.
9. The MinElute column was placed into a new 1,5ml collection tube and 14µl RNase free water were added to the center of the spin column membrane. Centrifugation (1min, full speed) followed.

10. The eluted RNA was stored at -20°C.

Testing the Kit:

For testing purposes 3 random pupae from each of the 3 genotypes served as samples. After following the kit protocol, the amount and quality of the RNA isolated was measured with a NanoDrop machine, the results can be seen in table 2.

Table 2: Concentration and quality of the RNA isolated using the kit measured with NanoDrop

	[RNA] [ng/µl]	**OD260/280**	**OD260/230**
w Met^{27}	44,6	2,1	0,84
y w	27,8	1,88	0,06
w gce^{2,5k}	23,7	2,09	0,58

cDNA synthesis was performed as described in the chapter "cDNA synthesis (Invitrogen)". 200ng RNA per sample were used for cDNA synthesis. The calculated volumes needed are shown in table 3.

Table 3: Volume of RNA solution needed for 200ng, final volume = 10µl

	RNA [µl]	**H$_2$O** [µl]
w Met^{27}	4,48	5,52
y w	7,19	2,81
w gce^{2,5k}	8,44	1,56

q-RT-PCR was performed using the iQ SYBR kit as described in the chapter "q-RT-PCR" with only using the Primer sets for the 2 housekeeping genes since the kit must give results for these genes for being usable in experiments. Another Primer set for a sequence which included an intron was used as well. cDNA does not include introns but gDNA does, so if there is gDNA contamination in the PCR product the length will be longer than expected for cDNA. Electrophoresis was done as described in chapter "Electrophoresis" which gave the results shown in figure 28.
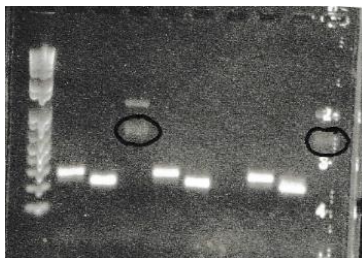

Figure 28: Testing the RNeasy kit electrophoresis results, order: Marker - y w + RP49 - y w + DmEcad – y w + intron primer – w Met^{27} + RP49 – w Met^{27} + DmEcad – w Met^{27} + intron primer – w gce^{2,5k} + RP49 – w gce^{2,5k} + DmEcad -w gce^{2,5k} + intron primer

The kit gave a rather low yield of RNA. The Electrophoresis Results show that RP49 and DmEcad gave the right products. Checking the cycle numbers and Melting curves gave normal results for the House-keeping genes. Later (higher) cycle numbers and unusual looking melting curves might stem from minor gDNA contamination, which would be verified by the size of the PCR product seen in the electrophoresis results. Figure 28 shows 2 different products, one of the cDNA and the other contamination with gDNA

which was marked with a black circle. The gDNA contamination seems minor and the other results are good. All results taken into account, the results show that the kit works.

RNA prep (Trizol)

This method used the protocol "Total RNA isolation and cDNA synthesis for RT-PCR from insect tissue or whole body" and was optimized for *Drosophila melanogaster*.

Procedure:

The chemicals and samples were kept on ice whenever they were not worked with.

1. The frozen pupae were homogenized in 0,5ml Trizol using a plastic pestle. Then another 0,5ml Trizol were added and the solution was vortexed briefly. The samples were then incubated at room temperature for 5min.
2. 0,2ml chloroform were added, then the samples were shaken by hand for 20sec. Incubation for 3min at RT followed.
3. Then the samples were centrifugated (12 000g, at 4°C, for 15min).
4. 0,5ml of the aqueous phase were transferred to a new tube and 450µl of isopropanol were added. Brief mixing and incubation for 10min at RT followed.
5. The samples were centrifugated again (12 000g, at 4°C, for 10min).
6. The liquid was discarded so only the pellet was left in the tube. As soon as all the liquid was removed from the pellet 1ml chilled 75% ethanol was added immediately. Brief vortexing followed.
7. The samples were then centrifugated (7500g, at 4°C, for 5min).
8. The liquid was discarded so only the pellet was left in the tube. After all the liquid was removed from the pellet 40µl nuclease-free water were added immediately. The samples were placed on ice while the pellet dissolved and occasionally vortexed.
9. Meanwhile a Turbo DNase (Ambion) premix was prepared, consisting of 14µl water, 6µl of 10x Turbo DNase buffer and 1µl Turbo DNase (for 1 reaction). For this water and buffer were combined first so the enzyme would not be destroyed in the pure water. The enzyme was the pipetted directly into the buffer and vortexed gently at low velocity.
10. When the RNA pellet was dissolved completely, 20µl of the Turbo DNase premix were added to each sample and mixed. The total volume was 60µl at this point.
11. The samples were then incubated in a 37°C water bath for 30min.
12. The next step was an extraction: 1 Volume (60µl) of a mixture of phenol, chloroform and isoamylalcohol in the ratio 25:25:1 was added. Centrifugation (full speed, 10min) followed.
13. 50µl of the phenol (upper phase) were transferred to a new tube. To get even more sample 50µl water were added to the original mixture of phenol, chloroform and isoamylalcohol as another extraction step.
14. 40µl of the water phase were transferred to the already extracted 50µl phenol phase resulting in a final volume of 90µl. Then 90µl of a mixture of chloroform and isoamylalcohol in the ratio 50:1 were added as the final extraction step. The mixture was shaken or vortexed until emulsion could be seen. Centrifugation (full speed, 10min) followed.
15. 65-75µl of the upper phase were transferred to a new tube. A tenth of this volume (6,5-7,5µl) of 3M Na-acetate (pH 5,2) were added to remove water which promotes precipitation. The solution was vortexed or shaken. Then about 180µl (2,5 volumes) of chilled 100% ethanol were added for precipitation.

16. Centrifugation to form the pellet (maximum speed, 15min) was followed by a washing step. First all the liquid was discarded, then 0,5ml 75% ethanol were added. The samples were vortexed briefly and then centrifugated for a few seconds.
17. All the liquid was discarded, and the RNA pellet was resuspended in 35μl water by vortexing.
18. The concentration and the quality of the isolated RNA could be determined with a NanoDrop machine. The RNA was stored at -20°C.

Testing the "Trizol Method":
The Samples used for the preliminary experiment were L, P, L2 and P2. Larvae (L) and pupae (P) were randomly selected with L, P and L2, P2 being from the same genotype. The result of using the Trizol method on these samples was measured with a nanodrop machine and can be seen in table 4.

Table 4: Concentration and quality of the RNA isolated with the Trizol Method measured with NanoDrop

	[RNA] [ng/μl]	OD260/280
L	283,8	2,04
P	430,6	2,05
L2	286,4	2,01
P2	328,4	2,04

Comparing the "Trizol method" to the RNeasy kit:
For the RNeasy kit less and a lower volume of substances were needed, and this method was also less time consuming. The RNA concentration resulting from the RNeasy kit is rather low compared to the concentration yielded by the Trizol method. The quality, which is derived from the OD280/260 ratio, that should be as close to 2,0 as possible, was better when isolation was done with the Trizol method. Also, the possible contamination with gDNA when using the RNeasy kit is a disadvantage.

cDNA synthesis (Invitrogen)
This method used the protocol "Total RNA isolation and cDNA synthesis for RT-PCR from insect tissue or whole body" and was optimized for *Drosophila melanogaster*.

Procedure:
Before cDNA synthesis the volume of RNA solution needed was calculated. This gave different volumes of RNA solution and water for each sample.

All chemicals and samples were kept on ice when they were not worked with.

The total volume of the reaction was 20μl. 10μl of individual Volume of RNA solution plus the individual volume of water were combined with 2μl Premix 1 and 8μl of Premix 2.

1. Premix 1 was prepared by adding 1μl of oligo(d)T primers to 1μl of 10mM dNTPs (for 1 reaction).
2. Individual volumes of water were transferred into 0,5ml tubes and individual volumes of RNA solution and 2μl Premix 1 were added
3. The samples were incubated in a 65°C water bath for 5 minutes. Then they were chilled on ice, centrifuged briefly, and placed back on ice afterwards.
4. For Premix 2 1μl nuclease-free water, 4μl 5x first-strand buffer (FS buffer), 2μl 0,1M DTT, 1μl SuperScript II and 1μl RNase OUT were combined.
5. 8μl of Premix 2 were added to the samples and mixed gently.

6. The samples were then incubated in a 42°C water bath for 50 minutes.
7. To stop the reaction by heat-inactivating the reverse transcriptase (SuperScript II), the samples were put in a 70°C water bath for 15 minutes, then chilled on ice, centrifuged briefly, and placed back on ice.
8. 1µl RNase H per reaction was added and the solution mixed before the samples were incubated again in a 37°C water bath for 20 minutes.
9. Finally, the samples were diluted to a 20x stock solution. 5µl of the original cDNA product were diluted to 100µl final volume.

Testing cDNA synthesis:

From the RNA isolated with the Trizol method a volume containing 2µg RNA was used for cDNA synthesis. Table 5 shows the calculations done before starting the procedure.

Table 5: Volume of RNA solution needed for 200ng RNA, final volume = 10µl

	RNA [µl]	H$_2$O [µl]
L	7,05	2,95
P	4.65	5,35
L2	6,98	3,02
P2	6,09	3,91

The method worked really well, and the cDNA synthesized this way was later used as sample for testing the primers and q-RT-PCR.

Primers

There were seven sets of primers used to identify the mRNA of AMPs for defense responses. The length of the PCR product would yield was calculated by aligning the Primers to the mRNA of the AMP. The source of all mRNA sequences were FASTA files obtained from NCBI. (NCBI, 2020)

Attacin-A (AttA)

NM_079021.5 Drosophila melanogaster Attacin-A (AttA), mRNA 790bp

AGTCAGCTCCAGCAATCCAGTTCAGCAACATGCAGAACACAAGCATCCTAATCGTGGCCCTGGTGGCACTTTTCGCCAT==TACCGAGGCACTTCC CACAACA==GGACCCATTCGCGTCCGTCGCCAGGTGCTCGGAGGTTCCTTAACCTCCAATCCCGCTGGTGGGGCTGATGCTCGTTTGGATCTGAC CAAGGGCATTGGCAATCCCAACCACAATGTGGTGGGTCAGGTTTTCGCCGCCGGAAACACTCAAAGTGGTCCAGTCACAACTGGCGGAACTTT GGC==CTACAACAATGCTGGTCATGGTGC==CTCTTTGACCAAAACACACACGCCCGGAGTGAAGGATGTTTTCCAGCAGGAGGCCCATGCCAATTT ATTCAACAATGGCAGACACAATCTGGATGCCAAGGTCTTTGCTTCGCAAAATAAACTGGCCAATGGTTTCGAGTTCCAGCGGAATGGAGCTGG TCTGGATTACTCCCACATCAACGGACATGGTGCTTCCTTGACGCACAGCAACTTCCCAGGAATCGGCCAGCAACTCGGCCTGGATGGACGTGC TAATCTCTGGTCATCGCCCAATCGTGCTACTACCTTGGATCTCACGGGATCGGCGAGCAAGTGGACGAGTGGACCGTTTGCCAACCAGAAGCC AAACTTTGGTGCTGGCCTGGGTCTATCTCATCATTTCGGCTAAGCCTGCGTATTTGATATTATTAATTCTAATTTATTGACAATTATATTAAAATC AAAATATTGAAACCTAATAAACCTAATAATAAATTTTAATTT

Primer Forward: ==TACCGAGGCACTTCCCACAACA== (position 80, 22bp long)

Primer Reverse: GCACCATGACCAGCATTGTTGTAG
in mRNA: ==CTACAACAATGCTGGTCATGGTGC== (position 284, 24bp long)

Length of PCR product: 228bp long

Attacin-D (AttD)

NM_079667 Drosophila melanogaster Attacin-D (AttD), mRNA 742bp
ACTCAAACTAAGAGATAGAGTGCAAGCAGAAAGACGAAATCAAAGAATTATATAAGATGGAATGTCAGGCTTCAGGAAAC
CCAAAGAGCGGAGCGGCAACCGCCCAATGCGGAGTAAGGGTCGGTGATGATCTTGCCAATGCTCGAGCCGGAGTATTCGC
CTCCACTCCAGGCGCTGGGGGTCCGGTCACCAAGGGAGTTTATG**GAGCGGTCAACGCCAATGGTC**ATGCACTCTCACTGC
AGCATGGCCACATCGAGGGCGTGGGCAGCACTACCACTGCCGCAGCCCAAGCCAATCTCTTCCAGAGCAATAACGCCGCT
CTGAATGCCACTGCATTTCACAGTCATAGCCGATCGCACGATCAGTTGGCGGAGGACTCAATTTGCAAACTGGAACGGG
TCACCAGGCGGCAGTGGGGGT**CACTAGGGTTCCTCAGTTCGGCA**TGACCGCCGTCCAGGCTTCTGGCACAGCAAATCTGT
ATACCTCTCCAAGTGGCAATCTCAACCTCAACGCCACCGGAAGTGCCAATCATCACCTCAGGGGACCGATGCGCGGCAAG
TCCGATTTCGGCACCGGAGTTAACTTGCGATATAATTTTTAAATCCTTTATAGTTTTATTGAAACTATTCATAGTCACAT
TTAGTACTTGCACGTAGCCAAGAAAAGAAACAAGTGCCGTATTTATATGCATTATATCGAAGATTAAATAAACCATGCTA
TTAAAAGCGCTTTCTACTTGGT

Primer Forward: **GAGCGGTCAACGCCAATGGTC** (position 405, 21bp long)

Primer Reverse: TGCCGAACTGAGGAACCCTAGTG
in mRNA: **CACTAGGGTTCCTCAGTTCGGCA** (position 422, 23bp long)

Length of PCR product: 240bp long

Cecropin-A (CecA)

NM_079849.4 Drosophila melanogaster cecropin A1 (CecA1), mRNA 339bp
CATCAG**TCGCTCAGACCTCACTGCAATA**TCAATATCTTTAGCTTCTCCTAAGAAAAAATCAAGAAAATAT
CACCATGAACTTCTACAACATCTTCGTTTTCGTCGCTCTCATTCTGGCCATCACCATTGGACAATCGGAA
GCTGGGTGGCTGAAGAAAATTGGCAAGAAA**ATCGAACGCGTTGGTCAGCA**CACTCGGGATGCCACAATCC
AGGGACTGGGAATCGCTCAACAAGCCGCCAATGTCGCCGCAACTGCCCGAGGTTGACCACGATGATTATT
TATAATTATTTATTTAAAGATCTATTTATTCTGTTGCTCCCTGTAAATAAAACAATTTT

Primer Forward: **TCGCTCAGACCTCACTGCAATA** (position 19, 22bp long)

Primer Reverse: TGCTGACCAACGCGTTCGAT
in mRNA: **ATCGAACGCGTTGGTCAGCA** (position 183 to 202, 20bp long)

Length of PCR product: 183bp long

Diptericin (Dpt)

NM_057460.4 Drosophila melanogaster diptericin A (DptA), mRNA 496bp
GTATCAGTCAGCATATTCCAGTTCTTCAATTGAGAACAACTGAGATGCAGTTCACCCATTGCCGTCGCCCTTAC**TTTGCTGC**
GCAATCGCTTCTACTTTGGCTTATCCGATGCCCGACGACATGACCATGAAGCCCACTCCACCACCGCAGTACCCACTCAA
TCTTCAGGGAGGCGGCGGTGGCCAGAGCGGCGATGGTTTTGGCTTTGCAGTCCAGGGTCACCAGAAGGTGTGGACCAGCG
ACAATGGACGCCACGAGATTGGACTGAATGGAGGATATGGACAGC**ACTTGGGAGGACCATATGGCAA**CTCAGAACCGAGC
TGGAAAGTGGGAAGCACCTACACCTACAGATTTCCGAATTTCTAAGCTTCATAAATATTTTATTGTAAAAAACTTCACCA
AATATTATCTCGATTGGTATCCGAGTCTAGCTATTATAAAAACCATACCCACTTTGTATATTCAGATAATTGCAAAATAT
ATAACCGAATACAACG

Primer Forward: **TTTGCTGCGCAATCGCTTCTAC** (position 73, 22bp long)

Primer Reverse: TTGCCATATGGTCCTCCCAAGT
in mRNA: **ACTTGGGAGGACCATATGGCAA** (position 286 to 307, 22bp long)

Length of PCR product: 234bp long

Metchnikovin (MTK)

NM_079028.3 Drosophila melanogaster metchnikowin (Mtk), mRNA 277bp

`GCATCAATCAATTCCCGCC`ACCGAGCTAAGATGCAACTTAATCTTGGAGCGATTTTTCTGGCCCTGCTGG
GTGTGATGGCCACGGCTACATCAGTGCTGGCAGAGCCTCATCGTCACCAGGGACCCATTTTCGATACGAG
GCCGTCGCCCTTCAA`TCCTAACCAACCAAGACCGG`GTCCAATTTATTAAATTGACAGTGGGAAATTCACA
CTGCTGATGTCGTTAACACATTGATAAAATTAATACAATTAAACCAAAACTGAACATC

Primer Forward: `GCATCAATCAATTCCCGCC` (position 10, 19bp long)

Primer Reverse: CCGGTCTTGGTTGGTTAGGA

in mRNA: `TCCTAACCAACCAAGACCGG` (position 165 to 184, 20bp long)

Length of PCR product: 174bp long

Defensin (Def)

NM_078948.3 Drosophila melanogaster defensin (Def), mRNA 405bp

TATTCCAAGATGAA`GTTCTTCGTTCTCGTGG`CTATCGCTTTTGCTCTGCTTGCTTGCGTGGCGCAGGCTC
AGCCAGTTTCCGATGTGGATCCAATTCCAGAGGATCATGTCCTGGTGCATGAGGATGCCCACCAGGAGGT
GCTGCAGCATAGCCGCCAGAAGCGAGCCACATGCGACCTACTCTCCAAGTGGAACTGGAACCACACCGCC
TGCGCCGGCCACTGCATT`GCCAAGGGGTTCAAAG`GCGGCTACTGCAACGACAAGGCCGTCTGCGTTTGCC
GCAATTGATTTCGTTTCGCTCTGTGTACACCAAAAATTTTCGTTTTTTAAGTGTCACACATAAAACAAAA
CGTTGAAAAATTCTATATATAAATGGATCCTTTTAATCGACAGATATTT

Primer Forward: `GTTCTTCGTTCTCGTGG` (position 21, 17bp long)

Primer Reverse: CTTTGAACCCCTTGGC

in mRNA: `GCCAAGGGGTTCAAAG` (position 235 to 250, 16bp long)

Length of PCR product: 229bp long

Drosocin (Dro)

NM_001259395.2 Drosophila melanogaster drosocin, transcript variant B (Dro), mRNA 754bp

```
AGTTCGATTTGTCCACCACTCCAAGCACAATGAAGTTCACCATCGTTTTCCTGCTGCTTGCTTGCGTTTT
TGCCATGGGTGTGGCCACTCCCGGCAAGCCACGCCCCTACAGCCCACGCCCCACCTCCCATCCCCGCCCC
ATTCGAGTGAGGCGCGAGGCACTGGCCATCGAGGATCACCTGACTCAAGCTGCCATCAGGCCACCACCCA
TTCTGCCCGCCTAAAGATGTGTGCATACCGCGGAGAAGTCATCCGATCAAATTTGTTTTGAAAAATCTTT
ATAAAAATTGTGAATTTTTTACTTTCTGCAAACAGTAAGCAATAAACACACGAAAGACAGCAATTAATAA
TCTTCAATCAATTGTGACACAATGAGGGGGTTCCCATCGCTTATCAGCGGTTTTTGTACCGAATCTGCTGA
GCTCTAGAGCTGATAAGAAATATACTTGCTCAAAACAAAACCACAAAAGTCACGTTTGAGAGAAAAAAG
CCTAAACGAATTTAATTCGCGACTCATATGAATCACAAACCTGTTCTATAGCACGTTCTTCTTAAATTCT
AGCGAAATAACCAGATGGCTGCAAATCATAATGAATGGGTTTGTCCCCTAAAAAAAACGAACTGACAAGC
CCCCTTATAAAACTTATTTATTAATAGATTAGTTCGTATATAATTGCATATGTAAATACTTTAAATAGAA
CAAATTATTACGACATTTAAAAATATATATCCTGGTTTTTAAAAACAGGGTTTG
```

Unfortunately, the Sequence of the Primers Dro For & Rev are not known to me and were not be tested in preliminary experiments.

House-keeping Genes

In addition, 2 different "Housekeeping genes" were targeted, E-cadherin (DmEcad) and Ribosomal protein (RP49), since they are present in all cell types and were therefore used as reference genes to the AMP genes.

Another advantage of RP49 as reference gene is that it is not affected by JH or JHa. (Flatt, et al., 2008)

Testing of the Primers

Before the Primers were used for the real experiment, they were tested to make sure they gave the correct product and which annealing temperature works best for the PCR.

RT-PCR (Emerald Amp Master Mix Kit):

For this preliminary test normal RT-PCR instead of q-RT-PCR was used. Table 6 lists the contents of 1 reaction.

Table 6: Master Mix content for 1 reaction, final volume = 25µl

Chemical	Volume [µl]
Emerald Amp Master Mix	12,5
Template	3
Primer Forward	0,25
Primer Reverse	0,25
dH$_2$O	9

As template the cDNA synthesized during the testing of the Method "cDNA synthesis (Invitrogen)" from the samples L, P, L2 and P2 was used. 6 AMP Primer sets for the AMP genes Att-A, Att-D, CecA, Dpt, MTK and Def, as well as both House-keeping genes were tested. Two different annealing temperatures were tested, 58°C and 62°C, since the annealing temperature must be carefully selected to fit both the Housekeeping gene Primers and the AMP Primers.

Electrophoresis:

For this preliminary test, Electrophoresis was performed with minor changes to the method used in the rest of the experiments.

For obtaining a 1,5% Agarose gel, 1,5g agarose were weighed in and dissolved in 100ml 0,5x TBE (Trisborate) buffer, then heated until the solution was clear and poured into the gel container. When the gel had solidified it was put in the electrophoresis chamber and covered in 0,5x TBE buffer. 4µl RT-PCR product and 5µl Marker were introduced into the gel wells, then between 80-100V were applied and the electrophoresis was run for about 40min.

In this case the gel was put into a container with water after electrophoresis was finished and 2µl GelRed dye were added for staining. The gel was stained for 20min and then rinsed with water. Pictures of the gel were then taken under UV-light exposure, resulting in figures 29 and 30. Figure 29 shows the results from PCR done with 58°C annealing temperature, while the results for PCR with 62°C annealing temperature can be seen in figure 30.
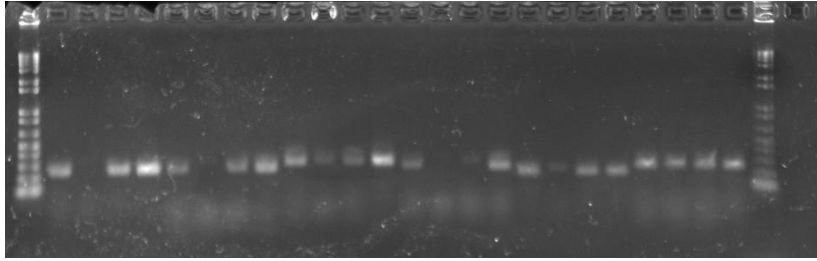
Figure 29: Annealing temperature: 58°C, Order: Marker, Att-A (L, P, L2, P2), Att-D (L, P, L2, P2), CecA (L, P, L2, P2), Dpt (L, P, L2, P2), MTK (L, P, L2, P2), Def (L, P, L2, P2), Marker
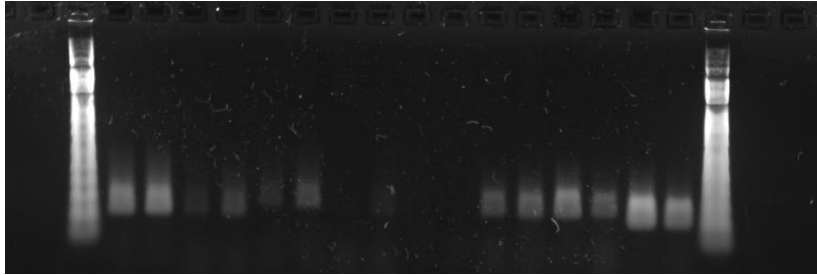
Figure 30: Annealing Temperature: 62°C, Order: Marker, Att-A (L2, P2), Att-D (L2, P2), CecA (L2, P2), Dpt (L2, P2), MTK (L2, P2), Def (L2, P2), DmEcad (L2, P2), RP49 (L2, P2), Marker

At 62°C there was no product for CecA and Dpt, but the results for both Housekeeping genes were good. For Att-A, Att-D, MTK and Def both temperatures gave good results for pupae tissue. Based on these results the annealing temperature of 58°C was used in the following experiments to ensure that all Primer sets were working properly.

To check which House-keeping gene was better suited as control value and which DNA sequences the Primers really gave, quantitative real time PCR was performed. The experiment was performed using the iQ SYBR kit as described in the chapter "q-RT-PCR". As template the cDNA of L2 and P2 were used and Primers for Att-A, Att-D, CecA, Dpt, MTK and Def as well as for both house-keeping genes were tested. All Primer sets gave good results. There were small differences between DmEcad and RP49, but both were deemed suitable control genes.

q-RT-PCR

For this Method the protocol and chemicals according to the protocol "q-RT-PCR using iQ SYBR kit (BioRad)" was used. Furthermore, Bio Rad PCR plates #HSP-9601 and Microseal® 'B' Adhesive Seals #MSB-1001 were used.

In each PCR done, 1 Master Mix contained the Housekeeping gene Primer sets as control for the AMP gene Primer sets. Two different PCR kits, one using iQ SYBR Green Supermix while the other uses TP 2x SYBR Master Mix, were used but both could be done according to the following procedure.

Procedure:
All chemicals used were kept on ice whenever possible.

1. First, a Master Mix was prepared for each set of primers used in the PCR. The contents of the Master Mix can be seen in table 7. Each Master Mix was mixed well by gently vortexing and then briefly centrifugated.

Table 7: Master Mix content for 1 reaction, final volume = 11µl

Chemical	Stock	Volume [µl]	Final concentration
dH$_2$O		3,3	
iQ SYBR or TP SYBR (Containing dNTPs and polymerase)	2x	7	1x
Primer Forward (0,1-0,5µM)	10µM	0,35	0,25µM
Primer Reverse (0,1-0,5µM)	10µM	0,35	10,25µM

2. 11µl of the Master Mix were transferred to each PCR plate well and 3µl of cDNA sample were added to each well. Every sample was run 3 times.
3. Then the plate was sealed and vortexed briefly.
4. The sealed plates could be stored at 4°C and they were centrifugated for 1min at full speed just before PCR was run.

q-RT-PCR program:
iQ SYBR contains a hot-start polymerase which required an initial heating step for activation. Antibodies that keep the polymerase inactive were destroyed in the heating process. The Program used for these experiments can be seen in table 8. The efficiency of the protocol should be 90-105%, the R^2 of the standard curve should be >0,98 and the Cq values received from the same sample should be similar.

Table 8: PCR cycle

Cycling Step	Temperature [°C]	Hold time (min:sec)	# of cycles
Initial DNA denaturation and polymerase activation	95	3:00	1
Denaturation	95	0:10 (0:10-0:15	
Annealing	55-64 (58 used in these experiments)	0:20 (0:15-0:30)	40
Extension	72	0:30	
Read			
Melt Analysis	55-95 (in 0,5°C increments)	0:10	1

Electrophoresis

For obtaining a 1% gel for a smaller number of samples, 0,5g agarose were mixed with 50ml of 0,5x TBE buffer. The mixture was heated until the solution was clear. The gel was then poured into the container and 2,5µl GelRed dye were added into the still liquid gel and distributed. After 20min the gel was solid and could be put into the electrophoresis chamber and flooded with 0,5x TBE buffer. 10µl of the samples (3µl PCR product + 2µl 10x loading buffer + 7µl H$_2$O) and the marker were applied to the wells. Then voltage of about 80V was applied for 30-45 minutes. For analysis a picture of the gel was taken under UV light.

Analysis of the PCR results

The quantification data (Cq values) gives the number of circles needed to get to the same amount of DNA amplified. If there's a lot of DNA present less circles are needed, when the amount of DNA is low, the number of circles increases, so the Cq value correlates to the amount of DNA present in the sample. The Housekeeping genes should give constant values. The same sample (which is processed 3 times) should give the same value, differing only in the second digit after the comma.

The melting curves are individual for each DNA segment, since every segment has an individual melting temperature depending on length and G/C and A/T content.

The Cq values were transferred to an Excel file where the Cq values of the AMP genes were normalized with the Cq values of the Reference gene (Housekeeping gene), both obtained from the same DNA sample, using the following formula:

$$\frac{Amplification^{Cq(Reference\ gene)}}{Amplification^{Cq(AMP\ gene)}}$$ With Amplifiction = Efficience = 2

For combining the data to one convincing value for the same sample the 3 Cq values of both the AMP gene and the Housekeeping gene were processed as follows:

1. Every Cq value of the AMP gene was combined with every Cq value of the Housekeeping gene using the formula mentioned above. This yielded 9 calculated values.
2. Then the arithmetic mean and the standard deviation from all 9 values was calculated.
3. The arithmetic mean for each AMP gene was then depicted in a bar chart.

Results

For this thesis three sets of experiments were used to show the influence of JH and its receptors on the immune system during metamorphosis in *D. melanogaster*. For investigating the immune response during metamorphosis, which is represented by AMP expression, developmental profiles for each AMP were compiled. The expression of AMPs was investigated in one wildtype-like genotype, *y, w*, and two mutated genotypes, *w, gce^{2,5k}* and *w, Met^{27}*, with unfunctional JH receptors. Furthermore, the direct influence of a JH analog on AMP expression in these genotypes was investigated. Lastly, genetically modified *D. melanogaster* should show the stage-specific AMP expression in all 3 genotypes *in vivo*.

Developmental profiles of AMP mRNA expression in control and JH receptor mutants

A set of samples was collected from the genotypes *y, w*, *w, gce^{2,5k}* and *w, Met^{27}* at chosen timepoints during metamorphosis. RNA isolation and cDNA synthesis were then followed by q-RT-PCR with Primer sets targeting several AMP genes and housekeeping genes for control.

Pupae from all three genotypes used for this experiment were collected 0h, 6h, 18h, 24h, 36h, 48h, 60h and 72h after the WP stage. RNA isolation was done using the RNeasy Plus Micro kit yielding RNA at concentrations between 5 and 42,9ng/μl and OD260/280 values ranging from 1,77 to 2,47. One sample yielded the very low amount of 2,4ng/μl with an OD260/280 value of 4,46. Every sample which yielded less than 10ng/μl was excluded from further processing. For cDNA synthesis according to the protocol "cDNA synthesis (Invitrogen)" described in the chapter "Methods" 150ng of RNA per reaction were used and the resulting cDNA was diluted to a 10x dilution with a final volume of 200μl. For q-RT-PCR the iQ

SYBR Green Supermix was used as described in the chapter "q-RT-PCR", each AMP gene Primer set was combined with 1 of the 2 Housekeeping gene Primer sets. Att-A was paired with DmEcad, while Att-D, CecA, Dpt, Def and MTK were paired with RP49.

Additional Pupae from all three genotypes were collected 18h, 30h, 36h, and 42h after the WP stage. RNA isolation was done using the Trizol method yielding RNA at concentrations between 125,4 and 303,1ng/µl and OD260/280 values ranging from 1,99 to 2,10. Every sample could be used for further processing. For cDNA synthesis according to the protocol "cDNA synthesis (Invitrogen)" described in the chapter "Methods" 1,25µg of RNA per reaction were used and the resulting cDNA was diluted to a 10x dilution with a final volume of 200µl. For q-RT-PCR the TP 2x SYBR Master Mix was used as described in the chapter "q-RT-PCR", each AMP gene Primer set was combined with 1 of the 2 Housekeeping gene Primer sets. Att-A, Att-D, CecA, Dpt, Def, MTK and Dro were all paired with RP49.

In figures 31-50 and tables 9-22 the results of the Electrophoresis and the summarized q-RT-PCR results obtained according to the descriptions in the chapters "Electrophoresis" and "Analysis of the PCR results" in "Methods" are shown.

Electrophoresis results

The order on the electrophoresis gels is the following:
First row: Marker-w $gce^{2,5k}$ 0h- w $gce^{2,5k}$ 6h- w $gce^{2,5k}$ 18h- w $gce^{2,5k}$ 24h- w $gce^{2,5k}$ 36h- w $gce^{2,5k}$ 48h - w $gce^{2,5k}$ 60h - w $gce^{2,5k}$ 72h - y w 0h
Second row: Marker- y w 6h - y w 18h - y w 24h - y w 48h - y w 60h - y w 72h -w Met^{27} 36h- w Met^{27} 60h - w Met^{27} 72h
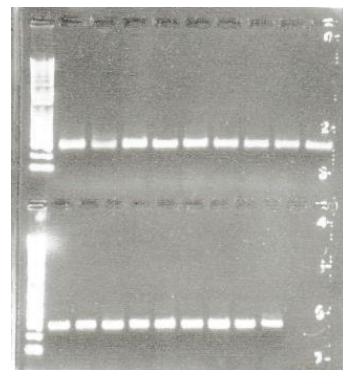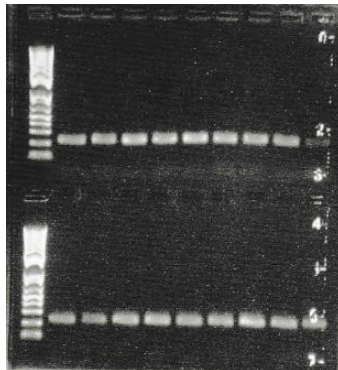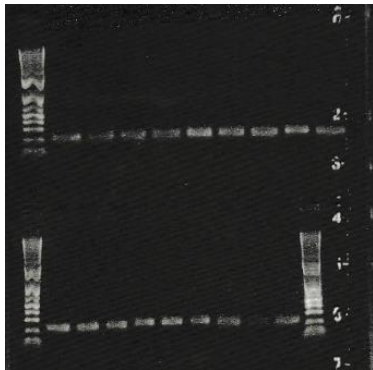
Figure 31: Electrophoresis results of Att-D   Figure 32: Electrophoresis results of Att-A Figure 33: Electrophoresis results of CecA
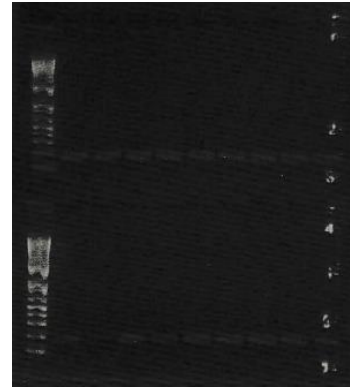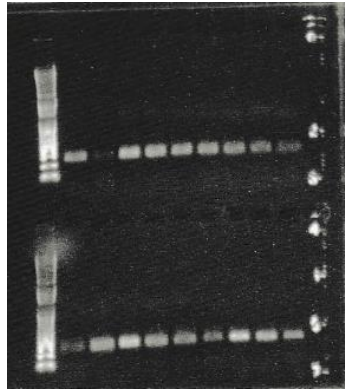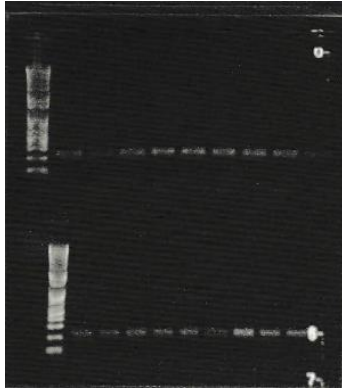
Figure 34:Electrophoresis results of Dpt   *Figure 35: Electrophoresis results of Def*   *Figure36: Electrophoresis results of MTK*

Figures 31 to 36 show the Electrophoresis gels exposed to UV light. The same PCR Products should have travelled to the same height in the gel. The electrophoresis results show that the q-RT-PCR indeed gave the same AMP product for each sample.

q-RT-PCR results

The first set of results included below in table 10-16 and figures 37-43 show AMP mRNA profiles from the genotype *y w*, in which AMP expression in a wildtype-like *Drosophila melanogaster* genotype is depicted over a course of 72 hours after the WP stage. High expression levels of the AMP investigated result in a peak at the specific timepoint and are marked yellow in the tables (>0,01). For analysing and comparing the results for the AMPs expressed in the genotype *y w*, I introduced a reference table, table 9, which assigns quantitative values to very high, high, moderate, low and very low expression levels, similar to what I found on FlyBase for depicting expression levels which can be seen in figures 6-25.

Table 9: reference table for the AMP expression levels

Very high	>0,1
High	>0,01
Moderate	>0,001
Low	>0,0001
Very low	<0,0001

Table 10: Values from the Att-A profile in the genotype *y w*

|	*y w*
Att-A 0h	0,01
Att-A 6h	0,92
Att-A 18h	12,06
Att-A 18h	0,05
Att-A 24h	0,81
Att-A 30h	0,01
Att-A 36h	0,01
Att-A 42h	0,003
Att-A 48h	1,33
Att-A 60h	0,40
Att-A 72h	0,11
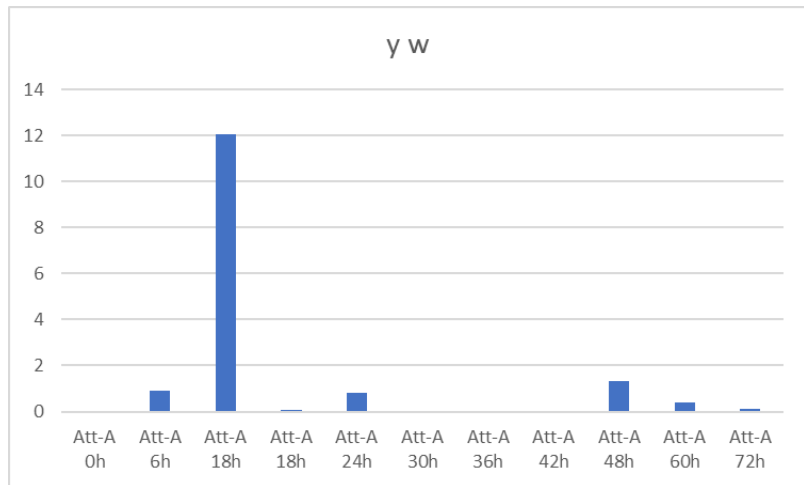
Figure 37: Depiction of Att-A profile from the genotype y w

The expression of Att-A in a wildtype-like background can be seen in Table 10 and its depiction in figure 37. Att-A is the only AMP gene that shows high expression in all but one timepoints. At 18h after WP stage, the Att-A expression reaches its highest peak. Alongside the 18h timepoint, also the timepoints 6h, 24h, 48h, 60h and 72h show very high expression levels. High expression can be seen for the WP stage, the second 18h sample, 30h and 36h, while at 42h the expression is considered moderate, the lowest Att-A expression in this profile.

Table 11: Values from the Att-D profile in the genotype *y w*

	y w
Att-D 0h	1,9594E-05
Att-D 6h	0,001
Att-D 18h	0,001
Att-D 18h	0,01
Att-D 24h	0,002
Att-D 30h	0,003
Att-D 36h	0,003
Att-D 42h	0,003
Att-D 48h	0,001
Att-D 60h	0,0003
Att-D 72h	0,0004
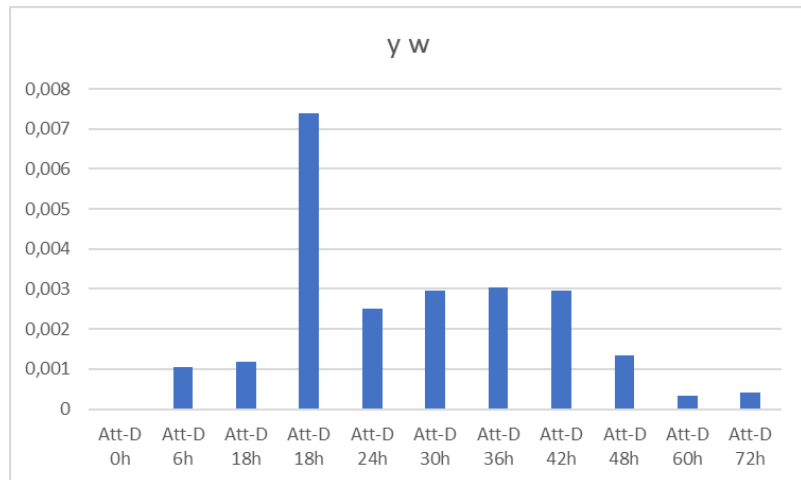
Figure 38: Depiction of Att-D profile from the genotype y w

The expression of Att-D in *y w* can be seen in Table 11 and is depicted in figure 38. At 18h after WP stage, the Att-D expression reaches its highest peak, which is also the only timepoint at which the expression is considered high. At most timepoints – namely 6h, the first 18h sample, 24h, 30h, 36h and 48h – the expression is moderate. 60h and 72h after WP stage, Att-D expression is low. At WP stage there is only very low expression observable. Except for the peak in the second 18h sample, Att-D expression seams to increase until it reaches a plateau at 30h and starts to decrease after 42h.

Table 12: Values from the CecA profile in the genotype *y w*

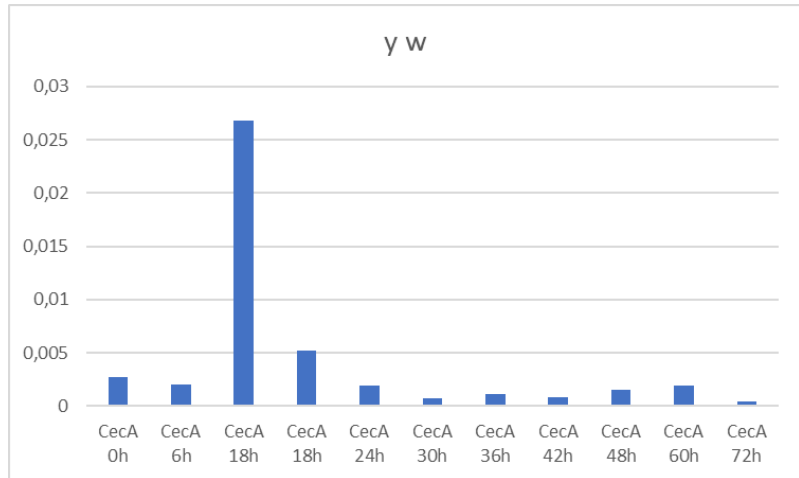|	*y w*
CecA 0h	0,003
CecA 6h	0,002
CecA 18h	0,03
CecA 18h	0,005
CecA 24h	0,002
CecA 30h	0,0007
CecA 36h	0,001
CecA 42h	0,0008
CecA 48h	0,001
CecA 60h	0,002
CecA 72h	0,0004

Figure 39: Depiction of CecA profile from the genotype y w

The expression of CecA in *y w* can be seen in Table 12 and figure 30 shows the depicted results. At 18h after WP stage, the CecA expression shows its highest expression peak, which is also the only timepoint at which the expression is considered high. Similar to Att-D, at most timepoints – namely 0h, 6h, the second 18h sample, 24h, 36h, 48h and 60h – the expression is moderate. 30h, 42h and 72h after WP stage, CecA expression is low. The lowest expression was found at the last investigated timepoint, 72h after WP stage.

Table 13: Values from the Def profile in the genotype *y w*

	y w
Def 0h	0,0002
Def 6h	0,0005
Def 18h	0,66
Def 18h	0,02
Def 24h	0,20
Def 30h	0,002
Def 36h	0,002
Def 42h	0,001
Def 48h	0,01
Def 60h	0,01
Def 72h	0,0006
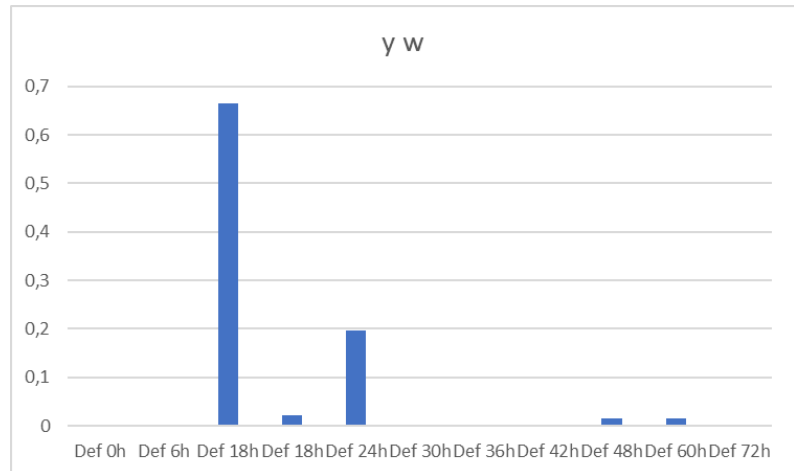
Figure 40: Depiction of Def profile from the genotype y w

The expression of Def in *y w* can be seen in Table 13 and is depicted in figure 40. At 18h after WP stage, the Def expression reaches its highest peak. 18h and 24h after WP stage, the expression is considered very high. High expression was found for the second 18h sample and at 48h and 60h. At the timepoints 30h, 36h and 42h moderate expression can be seen, and at 0h, 6h and 72h the expression stays low, with the lowest expression found at the WP stage.

Table 14: Values from the Dpt profile in the genotype *y w*

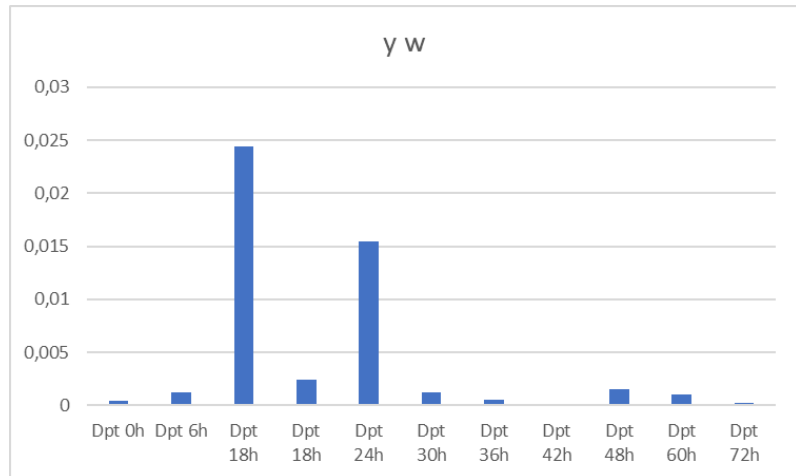|	*y w*
Dpt 0h	0,0004
Dpt 6h	0,001
Dpt 18h	<mark>0,02</mark>
Dpt 18h	0,002
Dpt 24h	<mark>0,01</mark>
Dpt 30h	0,001
Dpt 36h	0,0005
Dpt 42h	0,0001
Dpt 48h	0,001
Dpt 60h	0,001
Dpt 72h	0,0002

Figure 41: Depiction of Dpt profile from the genotype y w

The expression of Dpt in *y w* can be seen in Table 14 and is depicted in figure 41. At 18h after WP stage, the Dpt expression reaches its highest peak. 18h and 24h after WP stage, the expression was found to be high. Moderate expression can be seen for the second 18h sample, at 6h, 30h, 48h and at 60h. At the timepoints 0h, 36h, 42h and 72h low expression can be seen, with the lowest expression being at 42h.

Table 15: Values from the MTK profile in the genotype *y w*

	y w
MTK 0h	0,001
MTK 6h	0,0004
MTK 18h	0,002
MTK 18h	0,005
MTK 24h	0,0004
MTK 30h	0,0007
MTK 36h	0,003
MTK 42h	0,0009
MTK 48h	0,0001
MTK 60h	0,0009
MTK 72h	0,001
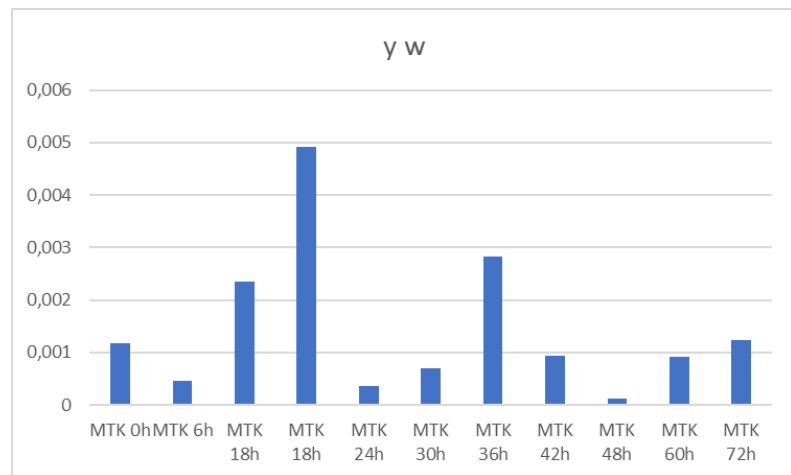
Figure 42: Depiction of MTK profile from the genotype y w

The expression profile of MTK in *y w* can be seen in Table 15 and its depiction in figure 42. At 18h after WP stage, the MTK expression reaches its highest peak. The AMP gene MTK shows no very high or high expression in any timepoint investigated. Moderate expression levels were found for both 18h samples and the timepoints 0h, 36h and 72h. At most timepoints – namely 6h, 24h, 30h, 42h, 48h and 60h – the MTK expression remained low. The lowest expression can be seen at 48h.

Table 16: Values from the Dro profile in the genotype *y w*

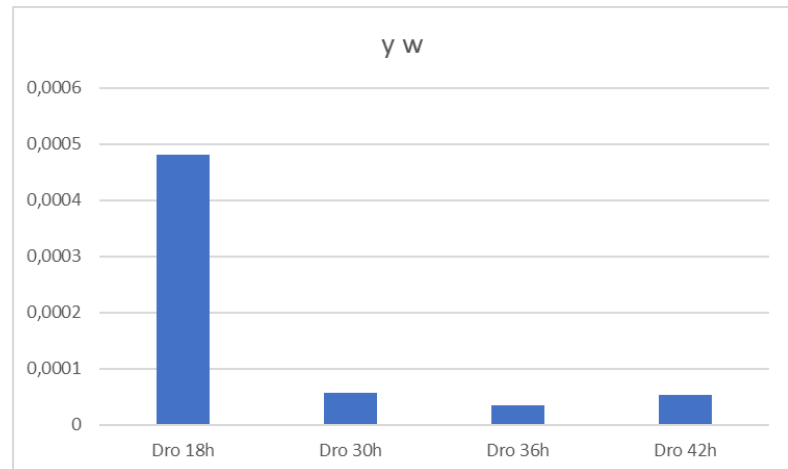|	*y w*
Dro 18h	0,0005
Dro 30h	5,6637E-05
Dro 36h	3,4453E-05
Dro 42h	5,2881E-05

Figure 43: Depiction of Dro profile from the genotype y w

The expression profile of Dro in *y w* is shown in Table 16 and is depicted in figure 43. At 18h after WP stage, the Dro expression reaches its highest peak, but the expression is considered low. Very low expression levels were observed for the other 3 investigated timepoints, 30h, 36h, and 42h. The lowest expression was found at 36h after WP stage.

The results show various levels of expression from 1,9594E-05 to 12,06. All AMP genes reach their highest expression at 18h after WP stage. Very high expression (> 0,1 peaks) can be seen at 0h for Att-A, at 6h for Att-A, at 18h for Att-A, Att-D, CecA, Def and Dpt, at 24h for Att-A, Def and Dpt, at 30h for Att-A, at 36h for Att-A, at both 48h and 60h for Att-A and Def, and at 72h for Att-A as well. This indicates that the natural expression of AMP genes varies strongly for each AMP and for each investigated timepoint. Att-A is the AMP with the highest expression levels throughout the AMP mRNA profile, while Dro was expressed at very low levels only.

Tables 17-23 and figures 44-50 show the results from AMP profiles from the genotypes *w gce^{2,5k}* and *w Met^{27}* compared to the values obtained from the *y w*. The values obtained from *w gce^{2,5k}* and *w Met^{27}* were divided by the corresponding value obtained from *y w* to result in the level of up- or downregulation compared to the wildtype-like genotype. Downregulation compared to the values from *y w* is marked red, while upregulation is marked green. Ten times the *y w* value (upregulation >10) is considered strong upregulation in a mutant genotype sample.

Table 17: Standardized values from the Att-A profile

	y w	*w gce^{2,5k}*	*w Met^{27}*
Att-A 0h	1	114,70	
Att-A 6h	1	1,31	
Att-A 18h	1	0,71	
Att-A 18h	1	1,30	0,14
Att-A 24h	1	1,87	
Att-A 30h	1	1,48	0,69
Att-A 36h		103,82	4475,80

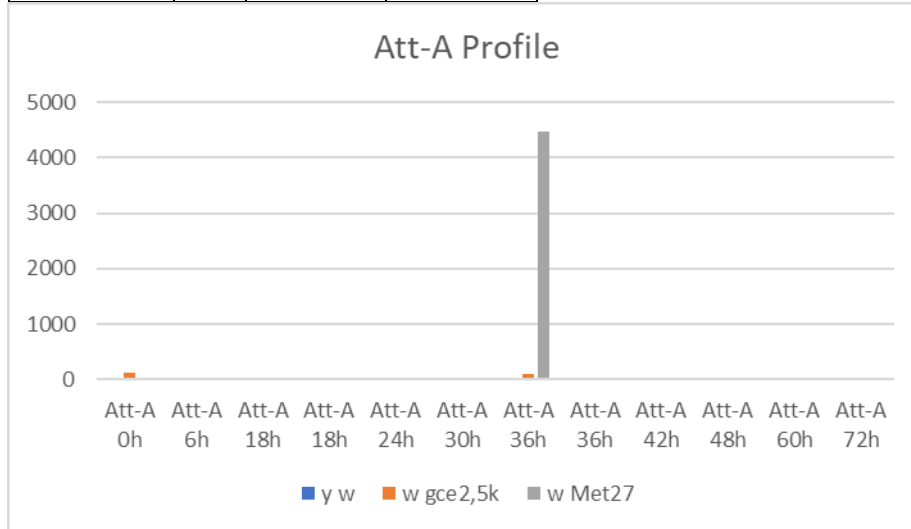|			
Att-A 36h	1	0,53	0,25
Att-A 42h	1	0,65	1,69
Att-A 48h	1	0,86	
Att-A 60h	1	1,46	0,55
Att-A 72h	1	2,65	1,45

Figure 44: Depiction of the Att-A profile results

Table 17 shows the Att-A expression in *w gce^{2,5k}* and *w Met^{27}* relative to the results obtained for Att-A expression in *y w,* the values are depicted in figure 44. Expression was strongly upregulated at 18h in the genotype lacking Gce and in one of the 36h samples for both mutated genotypes. In the *w gce^{2,5k}* genotype, upregulation can be seen for the timepoints 0h, 6h, 24h, 30h, 60h and 72h as well as in the first 36h sample and in the second 18h sample. Att-A expression in *w gce^{2,5k}* was downregulated compared to *y w* at the second 18h and 36h samples and 42h and 48h after WP stage. For the genotype lacking Met, upregulation of Att-A was observed at 42h and 72h and in one of the 36h samples, with the peak at 36h showing extremely strong upregulation, the strongest throughout all AMP profiles. Downregulation for *w Met^{27}* can be seen at 18h, 30h, 60h and the second 36h sample. Maximum upregulation of Att-A expression occurred at 36h in *w Met^{27}*, and maximum downregulation at 18h in *w Met^{27}* as well.

Table 18: Standardized values from the Att-D profile

	y w	*w gce^{2,5k}*	*w Met^{27}*
Att-D 0h	1	86,05	
Att-D 6h	1	9,66	
Att-D 18h	1	7,64	
Att-D 18h	1	1,74	0,12
Att-D 24h	1	2,07	
Att-D 30h	1	2,48	0,39
Att-D 36h		9,42	0,72
Att-D 36h	1	3,60	0,61
Att-D 42h	1	3,32	0,76
Att-D 48h	1	3,56	

Att-D 60h	1	11,31	2,58
Att-D 72h	1	4,03	0,46

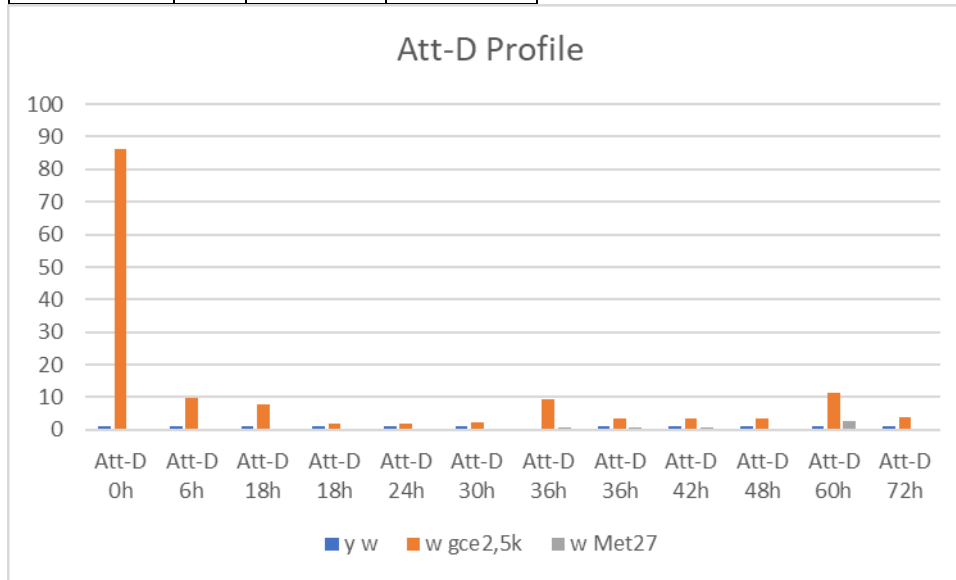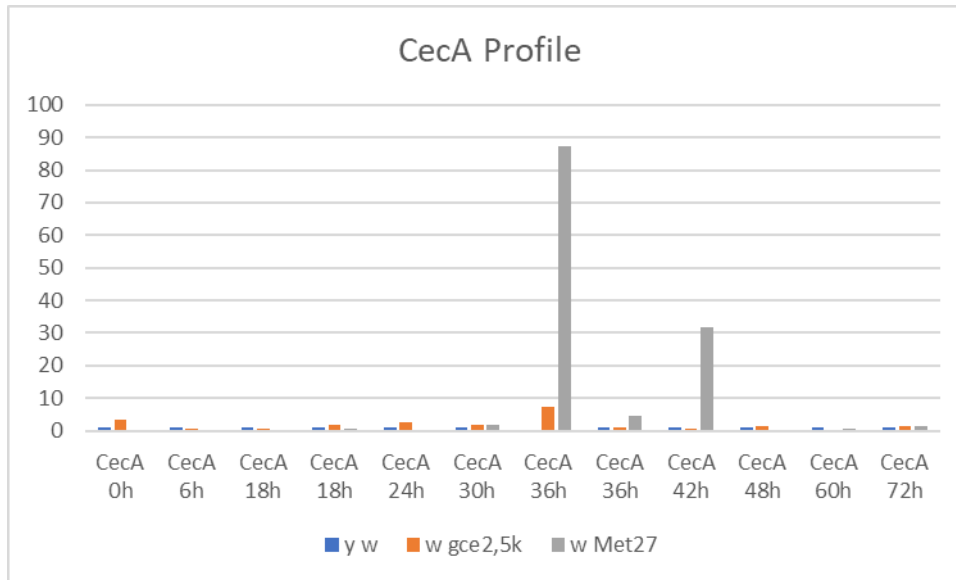*Figure 45: Depiction of the Att-D profile results*

Table 18 shows the Att-D expression in *w gce*[2,5k] and *w Met*[27] relative to the results obtained for Att-D expression in *y w,* the values are depicted in figure 45. Expression was strongly upregulated during the WP stage and 60h after the WP stage in the genotype *w gce*[2,5k]. For the genotype lacking the JH receptor Gce, upregulation was observed for all investigated timepoints. *w Met*[27] on the other hand showed downregulation of Att-D expression levels in all timepoints except for 60h after WP stage. Maximum upregulation of Att-D expression occurred at 0h in *w gce*[2,5k], and maximum downregulation at 18h in *w Met*[27].

Table 19: Standardized values from the CecA profile

	y w	*w gce*[2,5k]	*w Met*[27]
CecA 0h	1	3,51	
CecA 6h	1	0,83	
CecA 18h	1	0,78	
CecA 18h	1	1,99	0,70
CecA 24h	1	2,74	
CecA 30h	1	1,85	1,71
CecA 36h		7,43	87,24
CecA 36h	1	1,03	4,75
CecA 42h	1	0,72	31,70
CecA 48h	1	1,51	
CecA 60h	1	0,38	0,50
CecA 72h	1	1,55	1,30

Figure 46: Depiction of the CecA profile results

Table 19 shows the CecA expression in *w gce²,⁵ᵏ* and *w Met²⁷* relative to the results obtained for CecA expression in *y w,* the values are depicted in figure 46. Expression was strongly upregulated at 36h and 42h after WP stage in the genotype *w Met²⁷*. For the genotype *w gce²,⁵ᵏ*, upregulation was observed for the second 18h sample and 0h, 24h, 30, 36h, 48 and 72h after WP stage, while downregulation was found for the timepoints 6h, 42h, 60h and the first 18h sample. For *w Met²⁷* upregulation of the expression of CecA can be seen at 30h 36h, 42h and 72h after WP stage, while downregulation occurred at 18h and 60h. Maximum upregulation of CecA expression occurred at 36h in *w Met²⁷*, and maximum downregulation at 60h in *w gce²,⁵ᵏ*.

Table 20: Standardized values from the Def profile

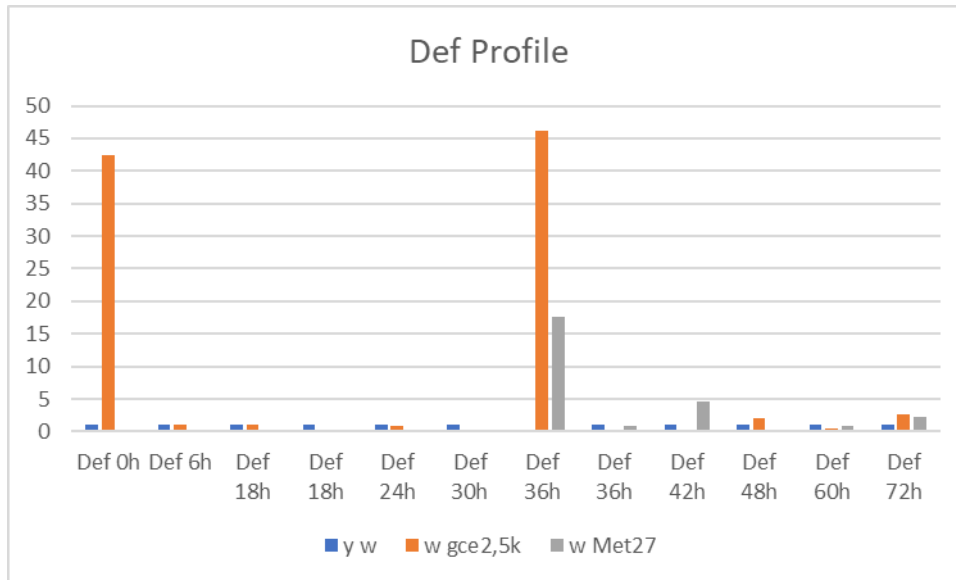|	*y w*	*w gce²,⁵ᵏ*	*w Met²⁷*
Def 0h	1	42,37	
Def 6h	1	1,01	
Def 18h	1	0,99	
Def 18h	1	0,04	0,29
Def 24h	1	0,95	
Def 30h	1	0,04	0,36
Def 36h		46,12	17,69
Def 36h	1	0,07	0,77
Def 42h	1	0,07	4,54
Def 48h	1	2,00	
Def 60h	1	0,41	0,89
Def 72h	1	2,59	2,28

Figure 47: Depiction of the Def profile results

Table 20 shows the Def expression in *w gce*^{2,5k} and *w Met*^{27} relative to the results obtained for Def expression in *y w,* the values are depicted in figure 47. Expression was strongly upregulated during the WP stage in *w gce*^{2,5k} and at 36h in both genotypes, *w gce*^{2,5k} and *w Met*^{27}. In *w gce*^{2,5k}, upregulation occurred at 0h, 6h, 48h, 72h and the first 36h sample. Downregulation for *w gce*^{2,5k} can be seen at the majority of the timepoints, namely 18h, 24h, 30h, 42h, 60h and the second 36h sample. For *w Met*^{27} upregulation of the Def expression was found at 42h and 72h after WP stage and the first 36h sample, while downregulation occurred at 18h, 30h and 60h and the second 36h sample. Maximum upregulation of Def expression occurred at 36h in *w gce*^{2,5k}, and maximum downregulation at 18h and 30h alike in *w gce*^{2,5k}.

Table 21: Standardized values from the Dpt profile

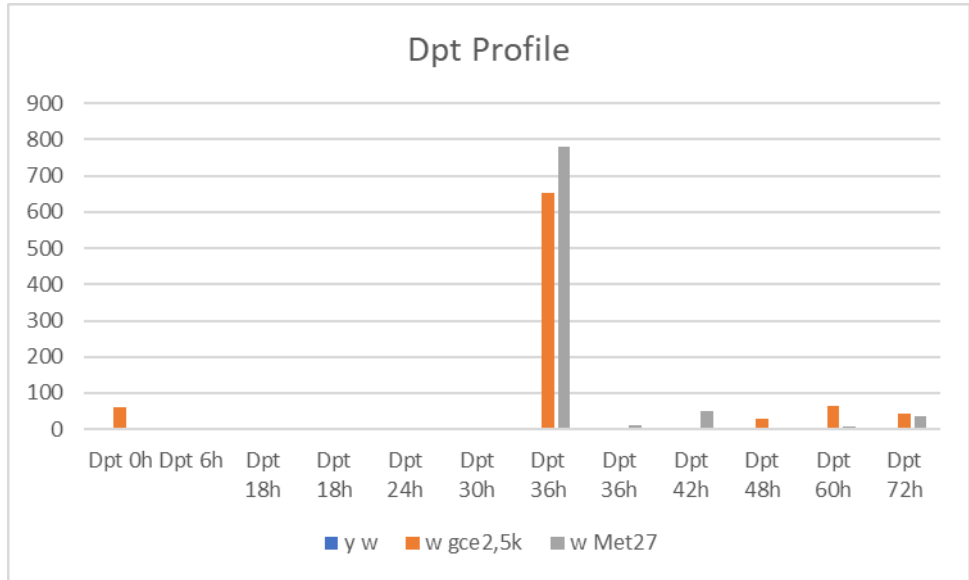|	*y w*	*w gce*^{2,5k}	*w Met*^{27}
Dpt 0h	1	60,82	
Dpt 6h	1	0,76	
Dpt 18h	1	5,71	
Dpt 18h	1	0,68	1,08
Dpt 24h	1	5,13	
Dpt 30h	1	0,50	1,93
Dpt 36h		652,85	781,86
Dpt 36h	1	3,53	11,61
Dpt 42h	1	1,46	51,79
Dpt 48h	1	30,54	
Dpt 60h	1	65,33	5,93
Dpt 72h	1	43,29	36,92

Figure 48: Depiction of the Dpt profile results

Table 21 shows the Dpt expression in *w gce^{2,5k}* and *w Met^{27}* relative to the results obtained for Dpt expression in *y w,* the values are depicted in figure 48. This AMP showed the most upregulated values compared to *y w* and the most strong upregulations are located in the Dpt profile as well. Expression was strongly upregulated during the WP stage and at 48h, 60h, 72h and in the first 36h sample in *w gce^{2,5k}*and 36h, 42h and 72h after WP stage in *w Met^{27}*. In *w gce^{2,5k}*, upregulation occurred at the majority of the timepoints, namely 0h, 24h, 36h, 42h, 48h, 60h, 72h and the first 18h sample. Downregulation for *w gce^{2,5k}* was found at 6h, 30h and the second 18h sample. For *w Met^{27}* upregulation of Dpt expression compared to *y w* was found at every timepoint investigated. Maximum upregulation of Dpt expression occurred at 36h in *w Met^{27}*, and maximum downregulation at 30h in *w gce^{2,5k}*.

Table 22: Standardized values from the MTK profile

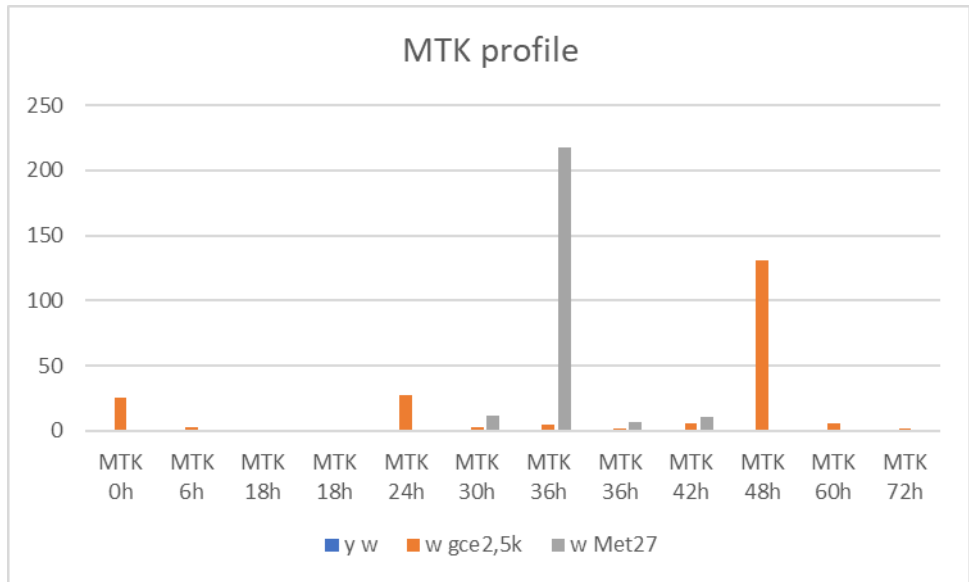|	*y w*	*w gce^{2,5k}*	*w Met^{27}*
MTK 0h	1	25,11	
MTK 6h	1	2,71	
MTK 18h	1	0,69	
MTK 18h	1	0,84	0,52
MTK 24h	1	27,52	
MTK 30h	1	2,99	11,42
MTK 36h		4,72	217,24
MTK 36h	1	1,66	6,84
MTK 42h	1	5,84	10,63
MTK 48h	1	130,96	
MTK 60h	1	5,48	0,51
MTK 72h	1	1,86	0,33

Figure 49: Depiction of the MTK profile results

Table 22 shows the MTK expression in *w gce^{2,5k}* and *w Met^{27}* relative to the results obtained for MTK expression in *y w,* the values are depicted in figure 49. Expression was strongly upregulated during the WP stage and at 24h and 48h in *w gce^{2,5k}* and 30h, 36h and 42h after WP stage in *w Met^{27}*. In *w gce^{2,5k}*, upregulation can be seen at all timepoints except for the downregulated MTK expression at 18h after WP stage. For *w Met^{27}* upregulation of MTK expression compared to *y w* was found at 30h, 36h and 42h after WP stage, while the expression levels were downregulated at 18h, 60h and 72h. Maximum upregulation of MTK expression occurred at 36h in *w Met^{27}*, and maximum downregulation at 72h in the genotype *w Met^{27}*as well.

Table 23: Standardized values from the Dro profile

	y w	*w gce^{2,5k}*	*w Met^{27}*
Dro 18h	1	0,66	0,17
Dro 30h	1	0,41	0,79
Dro 36h	1	0,55	1,25
Dro 42h	1	1,52	3,69
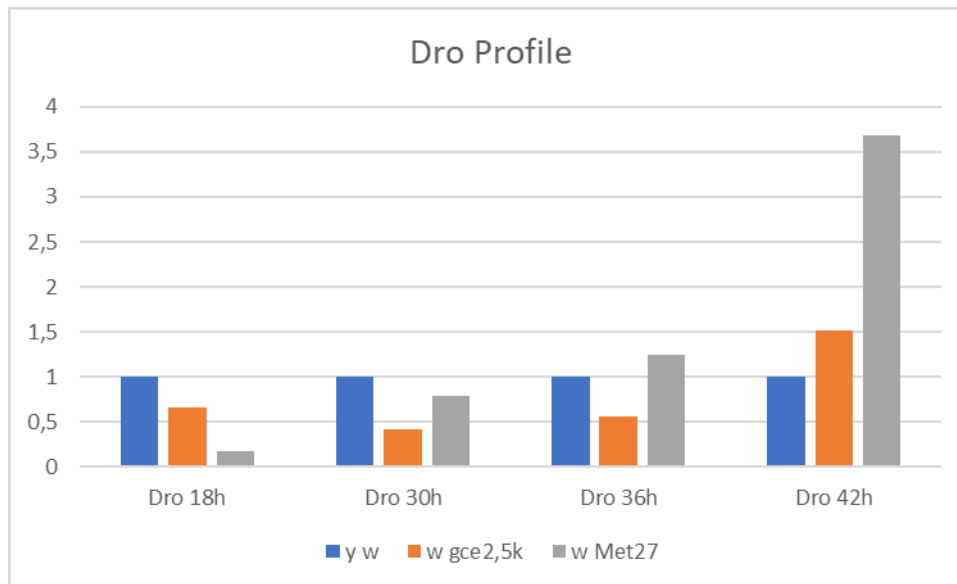
Figure 50: Depiction of the Dro profile results

Table 23 shows the Dro expression in *w gce^2,5k* and *w Met^27* relative to the results obtained for Dro expression in *y w,* the values are depicted in figure 50. There was no stron upregulation of Dro expression in any sample. In *w gce^2,5k*, upregulation was found for the timepoint 42h, while downregulation can be seen at 18h, 30h and 36h. For *w Met^27* upregulation of Dro expression compared to *y w* was found at half of the investigated timepoints, namely 36h and 42h, and downregulation could be observed at 18h and 30h. Maximum upregulation of Dro expression can be seen at 42h in *w Met^27*, and maximum downregulation at 18 in *w Met^27* as well.

Att-A is significantly upregulated 0h and 36h after WP stage in *w gce^2,5k* and 36h after WP stage in *w Met^27*. Among all timepoints investigated *w gce^2,5k* shows mostly a higher expression in Att-A compared to *y w*. Att-D shows significant upregulation in *w gce^2,5k* after 0h and 60h with Att-D always being higher expressed in *w gce^2,5k* than *y w* for all investigated timepoints, while downregulation was observed in *w Met^27* for most timepoints. CecA is significantly upregulated at 36h and 42h after WP stage in the *w Met^27* genotype. Both *w gce^2,5k* and w, *Met^27* have a higher expression of CecA than *y w* most of the time. Def is significantly upregulated at 0h and 36h in *w gce^2,5k* and at 36h in *w Met^27*. Both *w gce^2,5k* and *w Met^27* show a reduced expression of Def than *y w* in most timepoints. In the *w gce^2,5k* genotype Dpt is significantly upregulated at 0h, 36h, 48h, 60h and 72h after WP stage. In the w *Met^27* genotype Dpt is significantly upregulated at 36h, 42h and 72h after WP stage. Furthermore, w *Met^27* shows a higher expression of Dpt than the *y w* genotype at all timepoints, while in *w gce^2,5k* higher expression can only be observed at most of the timepoints. MTK is significantly upregulated 0h, 24h and 48h after the WP stage in *w gce^2,5k* and 30h, 36h and 42h after WP stage in w *Met^27*. *w gce^2,5k* shows mostly upregulation compared to *y w* for MTK, but mostly downregulation for Dro. Dro also shows no significant upregulation in any sample.

The results show a big variety of the degree to which AMP expression is up- or downregulated. Several timepoints show extremely high upregulation corresponding with only one of the JH receptors missing, indicating a crucial role od Gce and Met for the regulation of specific AMPs at specific timepoints. Met

seems to be crucial 36h after WP stage, while Gce seems to play an integral part at the events taking place during WP stage.

Effect of artificial JH on AMP mRNA expression

Three pupae from all three genotypes were collected 18h after being treated with PRX, a JHa, dissolved in acetone at the WP stage. Another three pupae from all three genotypes were treated with pure acetone and collected at the same age as control group. RNA isolation was done using the Trizol method yielding RNA at concentrations between 230,7 and 274,3ng/µl and OD260/280 values ranging from 1,80 to 2,07. Every sample could be used for further processing. For cDNA synthesis according to the protocol described in the chapter "Methods" 2µg of RNA per reaction were used and the resulting cDNA was diluted to a 10x dilution with a final volume of 200µl. For q-RT-PCR the TP 2x SYBR Master Mix was used as described in the chapter "q-RT-PCR", each AMP gene Primer set was combined with 1 of the 2 Housekeeping gene Primer sets. Att-A, Att-D, CecA, Dpt, Def, MTK and Dro were all paired with RP49. In figures 51-57and tables 24-30 the results of the q-RT-PCR are included.

q-RT-PCR results

All the values obtained from this experiment were compared to (by dividing by) the corresponding value of the wildtype-like genotype *y w* from the control group (C). This resulted in the ratio in which treatment with PRX influenced the AMP gene expression within each genotype as well as between all 3 genotypes.

Table 24: Att-A expression in samples treated with PRX (PRX) vs a control group (C)

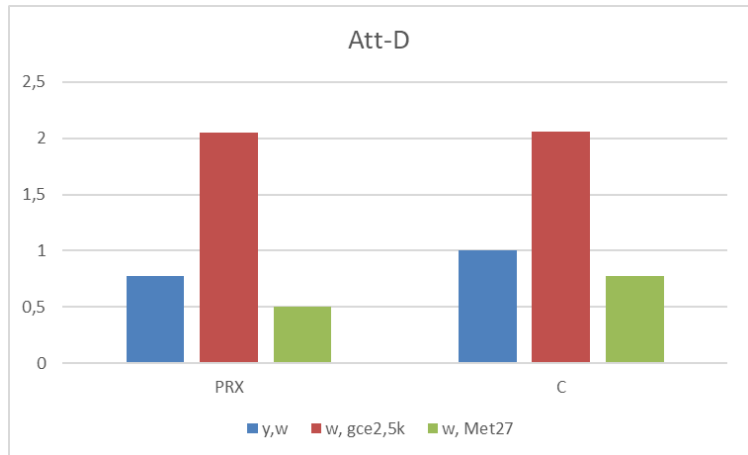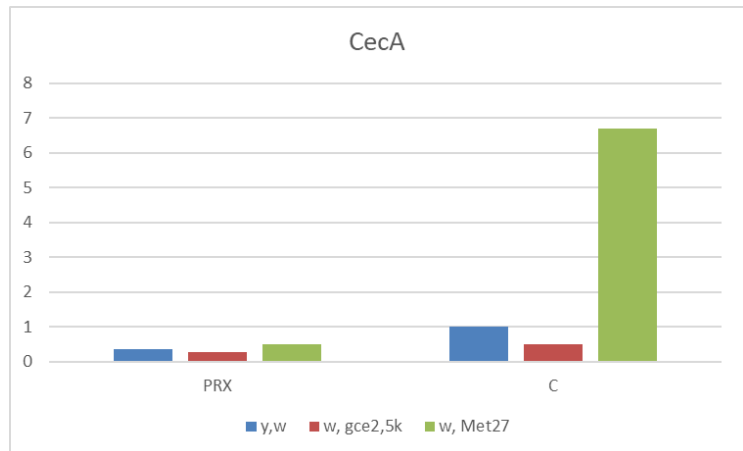|	*y w*	*w gce^{2,5k}*	*w Met^{27}*
PRX	0,28	0,17	0,09
C	1	0,14	0,17
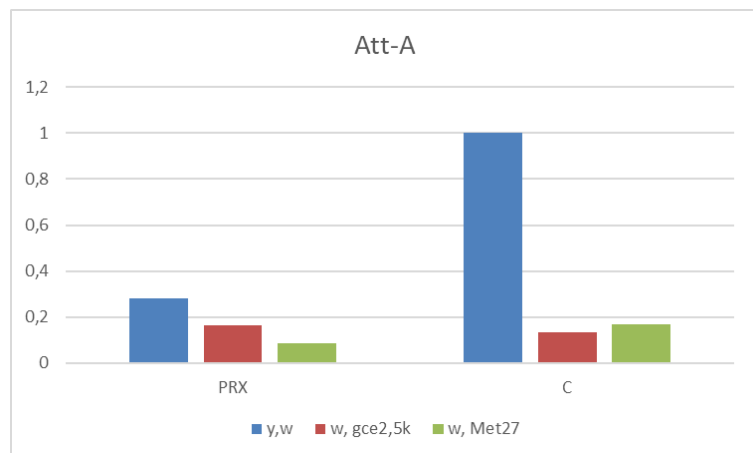
Figure 51: Depiction of Att-A expression in samples treated with PRX (PRX) vs a control group (C)

The expression of Att-A in all 3 genotypes was compared in 2 groups, one treated with PRX and the other treated with acetone as control group. The values relative to the *y w* control sample can be seen in table 24 and their graphic depiction in figure 51. Att-A was suppressed by 72% in *y w* after treatment with PRX. In *w gce^{2,5k}*, Att-A expression increases slightly, while in w *Met^{27}* expression almost halves.

Table 25: Att-D expression in samples treated with PRX (PRX) vs a control group (C)

	$y\ w$	$w\ gce^{2,5k}$	$w\ Met^{27}$
PRX	0,78	2,05	0,50
C	1	2,06	0,77

Figure 52: Depiction of Att-D expression in samples treated with PRX (PRX) vs a control group (C)

The expression of Att-D in all 3 genotypes was compared between samples treated with PRX and control samples. The values relative to the *y w* control sample can be seen in table 25 and their graphic depiction in figure 52. Att-A was suppressed by 22% in *y w* after treatment with PRX. In *w gce^{2,5k}*, Att-A expression did not change, while in w *Met^{27}* expression was lowered.

Table 26: CecA expression in samples treated with PRX (PRX) vs a control group (C)

	$y\ w$	$w\ gce^{2,5k}$	$w\ Met^{27}$
PRX	0,37	0,27	0,51
C	1	0,50	6,68

Figure 53: Depiction of CecA expression in samples treated with PRX (PRX) vs a control group (C)

The expression of CecA in all 3 genotypes was compared between samples treated with PRX and control samples. The values relative to the *y w* control sample can be seen in table 26 and their graphic depiction in figure 53. CecA was suppressed by 63% in *y w* after treatment with PRX. In *w gce^{2,5k}*, Att-A expression almost halved, while in w *Met^{27}* expression strongly reduced.

Table 27: Def expression in samples treated with PRX (PRX) vs a control group (C)

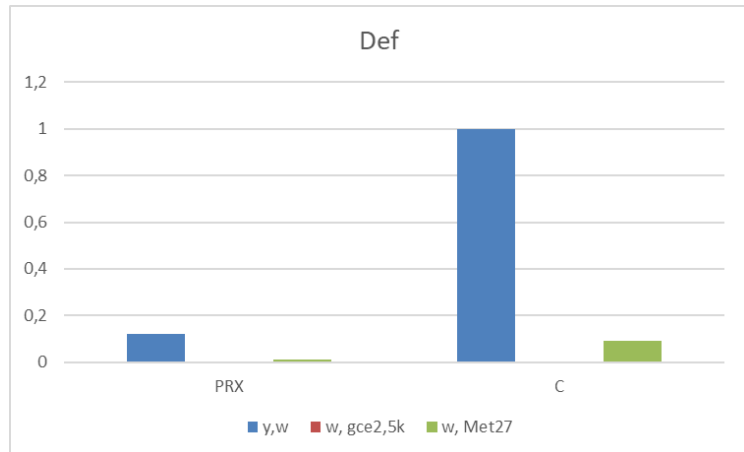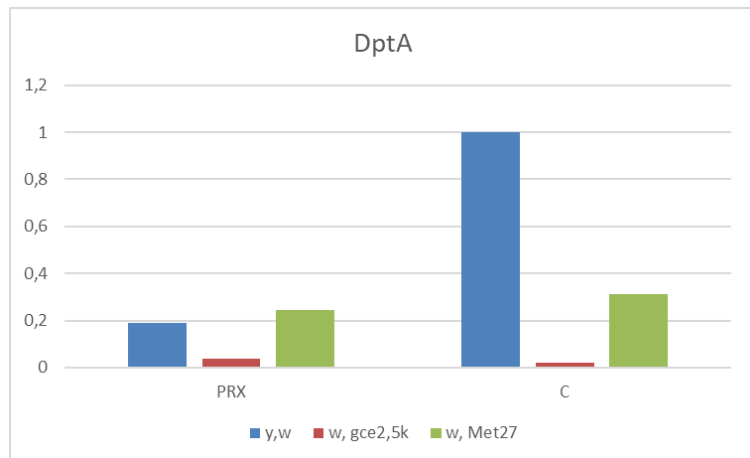|	*y w*	*w gce²,⁵ᵏ*	*w Met²⁷*
PRX	0,12	0,0015	0,012
C	1	0,005	0,090

Figure 54: Depiction of Def expression in samples treated with PRX (PRX) vs a control group (C)

The expression of Def in all 3 genotypes was compared between samples treated with PRX and control samples. The values relative to the *y w* control sample can be seen in table 27 and their graphic depiction in figure 54. Def expression was suppressed by 88% in *y w* after treatment with PRX. In both *w gce²,⁵ᵏ* and *w Met²⁷*, Att-A expression was reduced upon PRX application.

Table 28: Dpt expression in samples treated with PRX (PRX) vs a control group (C)

	y w	*w gce²,⁵ᵏ*	*w Met²⁷*
PRX	0,19	0,035	0,24
C	1	0,019	0,31

Figure 55: Depiction of DptA expression in samples treated with PRX (PRX) vs a control group (C)

The expression of Dpt in all 3 genotypes was compared between samples treated with PRX and control samples. The values relative to the *y w* control sample can be seen in table 28 and their graphic depiction in figure 55. Def expression was suppressed by 81% in *y w* after treatment with PRX. In *w gce²,⁵ᵏ* Dpt expression almost doubled after PRX application, while Dpt expression was reduced in *w Met²⁷*.

Table 29: MTK expression in samples treated with PRX (PRX) vs a control group (C)

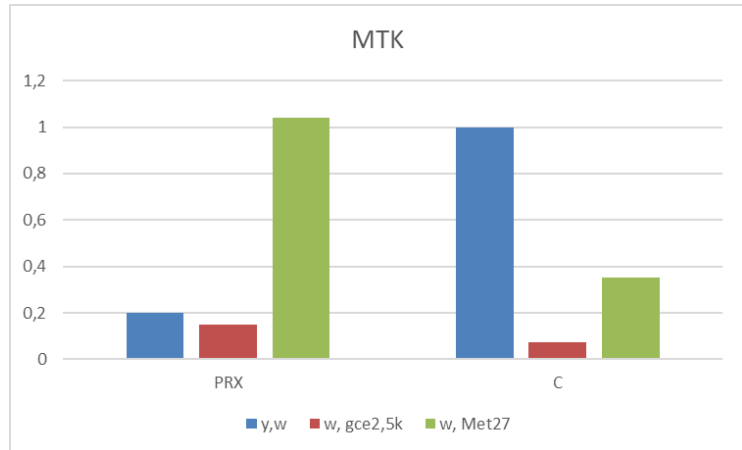|	*y w*	*w gce²,⁵ᵏ*	*w Met²⁷*
PRX	0,20	0,15	1,04
C	1	0,074	0,35

Figure 56: Depiction of MTK expression in samples treated with PRX (PRX) vs a control group (C)

The expression of MTK in all 3 genotypes was compared between samples treated with PRX and control samples. The values relative to the *y w* control sample can be seen in table 29 and their graphic depiction in figure 56. MTK expression was suppressed by 80% in *y w* after treatment with PRX. In *w gce²,⁵ᵏ* MTK expression almost doubled after PRX application, while the expression almost tripled in *w Met²⁷*.

Table 30: Dro expression in samples treated with PRX (PRX) vs a control group (C)

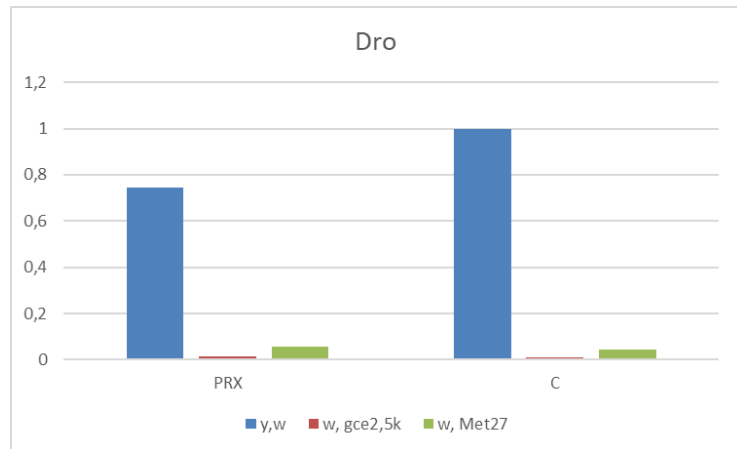|	*y w*	*w gce²,⁵ᵏ*	*w Met²⁷*
PRX	0,74	0,015	0,058
C	1	0,012	0,042

Figure 57: Depiction of Dro expression in samples treated with PRX (PRX) vs a control group (C)

The expression of Dro in all 3 genotypes was compared between samples treated with PRX and control samples. The values relative to the *y w* control sample can be seen in table 30 and their graphic depiction in figure 57. MTK expression was suppressed by 26% in *y w* after treatment with PRX. In *w gce²,⁵ᵏ* Dro expression slightly increased, the expression increased in *w Met²⁷* as well.

In the genotype *y w* treatment with PRX leads to all peaks being reduced, but the effect has not the same strength in all AMP genes. Strong reduction in AMP expression can be seen for Att-A, Def, Dpt and MTK.

In the *w gce*^{2,5k} genotype, treatment with PRX has none or only little effect. Expression peaks are slightly higher than in the control group for Att-A and for the AMP genes MTK and Dpt expression has even doubled. Expression is slightly reduced in Def and CecA while there is no notable difference in Att-D and Dro expression levels.

For *w Met*^{27} the AMP expression was most often lowered after PRX was applied. Significant downregulation can be seen for CecA. There was a slight increase after PRX treatment in the expression of Dro, and even a strong upregulation in MTK after PRX application.

Expression of transgenic AMP reporter constructs *in vivo*

Unfortunately, this experiment did not go as well as expected. The few pupae that could be collected and observed showed AMP-GFP expression under UV light, but we were unable to see a strong enough GFP signal to evaluate the data. No pattern regarding timepoint, location or gender could be detected. The visual readout was too weak to permit any conclusions about the effect of JH on AMP expression. This was an unfortunate technical problem beyond our control. The planned western blotting was not performed due to the lack of indications regarding notable timepoints or specific targets to investigate that could have been derived from GFP expression levels.

Discussion

The results of the performed experiments showed a rather large variability of AMP expression levels regarding both the time profile during metamorphosis and the genotype. Furthermore, the effect of application of a JH analogue differed with a wide range of AMP expression among all genotypes. Below, I will discuss the trends that were found by analysing the results, possible explanations and previous findings from other studies comparable to my experiments.

Developmental profiles of AMP mRNA expression in control and JH receptor mutants

AMP mRNA profiles over a course of 72h after WP stage were done in the backgrounds of only one of the two JH receptors being functional, either *w Met*^{27} or *w gce*^{2,5k}, and the *w* genotype with fully functional JH signalling with both receptors as control. The results of AMP expression in JH receptor mutants were then compared to the *w* control.

My findings:

Even though the expression levels in the AMP profiles were diverse, the trend of upregulation when there is no functional JH signalling due to a missing mediator, is clearly visible and expected, since JH is a known immune suppressor. (Jindra, et al., 2015) (Flatt, et al., 2008) (Schwenke & Lazzaro, 2017)

The dominant effect of Gce as main mediator for immune regulation by JH can be discerned from my results as well. (Jindra, et al., 2015)

Att-A
For Att-A the genotype *y w* shows naturally high expression levels, but especially 0h and 36h after WP stage Gce and Met have a big influence with Att-A suppression being reduced drastically when one JH receptor is missing.

Att-D
The genotype *w gce*^{2,5k} gives very high expression levels for Att-D at the timepoints 6h, 18h, 30h, 36h and

42h while expression in the genotypes *y w* and *w Met^27* remains low. Att-D appears to be sensitive to the loss of Gce in particular.

CecA

w Met^27 shows high expression levels for CecA at 36h while expression in *w gce^{2,5k}* and *y w* remains low at that timepoint. Similarly, expression of CecA in *w Met^27* is also very high at 42h with *y w* showing a reduced and *w gce^{2,5k}* no peak.

Dpt

High Dpt expression can be seen in *w Met^27* after 18h, 30h, 36h and 42h, with lowered expression levels in *y w* and *w gce^{2,5k}*. At 18h after WP stage expression of Dpt expression is increased in *w gce^{2,5k}* but not in *y w*. Dpt is more sensitive to the loss of the Met protein.

Def

Peaks of Def expression can be observed at 24h in *w gce^{2,5k}* and *y w* at a similar level. At 36h *w gce^{2,5k}* shows moderate Def expression while no peak can be seen for *w Met^27*. High and moderate expression levels can be seen for *y w* and *w Met^27* respectively at 18h.

MTK

18h after WP stage *y w* shows the highest, *w gce^{2,5k}* moderate and *w Met^27* lowered MTK expression levels. At 30h, 36h and 42h *w Met^27* shows high expression of MTK, with *w gce^{2,5k}* and *y w* showing lower expression levels.

Dro

At 18h after WP stage *y w* gives the highest expression levels, with *w gce^{2,5k}* following closely behind and *w Met^27* showing reduced levels. At 42h though, *w Met^27* shows the highest, *w gce^{2,5k}* moderate and *y w* lowered levels of Dro expression.

The results regarding JH receptor mutation are summarized in tables 31 and 32 below.

Table 31: Unfunctional Gce receptor, *w gce^{2,5k}*, relative to *y w*

AMP	Strong upregulation	Overall regulation
Att-A	0h, 36h	upregulation
Att-D	0h, 60h	upregulation
CecA	-	upregulation
Def	0h, 36h	downregulation
Dpt	0h, 36h, 48h, 60h, 72h	upregulation
MTK	0h, 24h, 48h	upregulation
Dro	-	downregulation

Table 32: Unfunctional Met receptor, *w Met^27*, relative to *y w*

AMP	Strong upregulation	Overall regulation
Att-A	36h	downregulation
Att-D	-	downregulation
CecA	36h, 42h	upregulation
Def	36h	downregulation
Dpt	36h, 42h, 72h	upregulation

MTK	30h, 36h, 42h	upregulation
Dro	-	-

When comparing the same samples from the timepoints 18h and 36h the fact that peaks are not consistent stands out. 4 expression peaks present in one sample were missing in the other. A possible explanation is that the genes could be very sensitive to stress and that peaks are not immune or developmental responses, but stress responses that occurred in only one of the 2 samples. It could also be explained with a bacterial infection of one vial from which the sample was taken or by some systematic or random error or a contamination of the sample.

Comparison of the results with data from different sources

The temporal expression levels for Att-A are shown in figure 8. Moderate expression levels can be seen for the WP stage, high expression was found 24h after WP stage, pupae 48h after the WP stage showed moderate expression and low expression levels can be seen for 72h after WP stage. In my Att-A expression results obtained from the *y w* genotype, the peak for 0h and 24h was lower than in figure 8, with the expression levels for 48h and 72h being at a comparable level.

Att-D temporal expression levels are depicted in figure 11. Moderate expression levels can be seen for the WP stage, and for 24h and 48h after the WP stage, while there were only very low expression levels for 72h after WP stage. My Att-D expression results from the *y w* genotype show almost no expression and lower expression at 0h and 48h, respectively. The expression levels for 24h and 72h are at a comparable level.

Figure 13 shows moderate expression levels for CecA1 at 0h, 24h and 48h after WP stage, and very low expression after 72h. These finding match the CecA1 expression I found for *y w.*

Def temporal expression levels are depicted in figure 16. Moderate expression levels can be seen for the WP stage, for 24h the expression is moderately high, 48h after the WP stage the expression reduces to moderate levels and there was only very low expression for 72h after WP stage. My Def expression results from the *y, w* genotype show almost no expression at WP stage, while the expression levels for 24h, 48h and 72h after WP stage are at a comparable level.

The temporal expression levels of Dpt shown in figure 19 are very high for 0h, 24 and 48h after WP stage and still high at 72h after WP stage. 24h shows the highest expression followed by 0h, then 48h and 72h shows the lowest expression. In my results for Dpt expression in *y, w* there was almost no expression at 0h and 72h after WP stage, while my results showed a lower expression at 48h than at 24h after WP stage as well.

MTK expression depicted in figure 22 shows very high levels at WP stage and 24h after WP stage. The expression levels then decreased to high and moderate for 48h and 72 after WP stage, respectively. My Def expression results from the *y w* genotype shows a peak at WP stage but no very high expression. The other expression levels do not match my results either. At 24h after WP stage the expression levels I found were very low. My results show a reduction from 24h to 48has in figure x, but the expression level is still lower. 72h after WP stage the expression should have reduced further, but the expression levels at 72h are actually higher than for 24h and 48h in my results but might match the description of a "moderate" expression.

Dro expression could not be compared since the timepoints of the previous results did unfortunately not overlap with my experiment.

The data shown in figure 58 were obtained from previous experiments similar to the setup of the experiments performed for this thesis. The data was provided by Dr. Marek Jindra was not published. The peak of Att-A expression at 18h can be seen in both the previous experiment and the results for *y, w* in this thesis. Expression of Att-A also matches in the timepoints 6h, 24h and 30h after WP stage. 48h, 60h and 72h show a higher while 36h and 42h show lower expression.
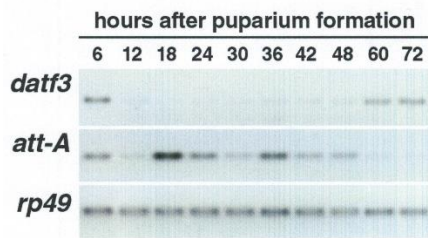
Figure 58: Data of a previous experiment including Att-A, rp49 and datf3 expression profiles

Since the comparison of my results for AMP expression in the *y w* genotype to previous experiments and a reliable source shows many inconsistencies, the reliability of the found AMP expression levels in the other genotypes is questionable as well.

Impact of JH receptor and timepoint during Metamorphosis

When the JH receptor mediating the AMP suppression is genetically removed, the expression of AMPs should increase. When functional Gce is missing, 5 of 7 AMP genes show a higher expression, which indicates that JH signaling is dependent on Gce as the main receptor as stated by Jindra et al. (Jindra, et al., 2015) Def and Dro show the opposite effect with being downregulated when Gce is missing, these two AMPs could be examples for immune response genes induced by JH signalling which was suggested by Flatt at al. (Flatt, et al., 2008) During the WP stage (0h), AMP expression is significantly raised in 5 of 7 investigated AMP genes in the w *gce*^{2,5k} genotype compared to the *y, w* genotype. It seems like the downregulation of an immune response or a developmental event is dependent on the presence of Gce. Att-D shows a higher expression when Gce is absent in all timepoints investigated.

When Met is absent, the investigated AMPs are either down- or upregulated in equal number. This suggest that some AMPs can be suppressed over Met, even when Gce is still functional. This would contradict the assumption that Met does not have a role in development and that immunity is independent of Met. (Flatt, et al., 2008) (Jindra, et al., 2015) 36h after the WP stage the level of AMP expression is significantly raised in 5 of 7 investigated AMP genes in the *w Met*^{27} genotype, suggesting that Met is crucial for JH signalling in this timepoint. When Met is missing, Dpt shows a higher expression than in *y w* at every timepoint investigated.

Att-A and Att-D show different regulation even expression though the proteins are similar. (FlyBase, 2020)

Att-A and Att-D are mostly upregulated in *w gce*^{2,5k} while they are mostly downregulated in *w Met*^{27}, suggesting their suppression by JH is mainly mediated by Gce. MTK, Dpt and CecA show upregulation when both JH receptors are absent, hinting at the possibility that both Met and Gce are part in the downregulation process. Dro gave no clear results for the absence of either gene. Def, on the other

hand, was downregulated in both *w gce*[2,5k] and *w Met*[27]. This can be explained by Def being induced rather than suppressed by JH signals mediated by both Met and Gce, maybe in a developmental role since Def is expressed during metamorphosis without an infection being present. (FlyBase, 2020)

All investigated AMPs which are suppressed by JH signalling mediated by Gce are Anti-Gram-negative AMPs - AttA, AttD, CecA1, DptA and Dro. There does not seem to be a pattern regarding if the AMPs are regulated by the IMD or the Toll pathway. (FlyBase, 2020) (FlyBase, 2020) (FlyBase, 2020) (FlyBase, 2020) (FlyBase, 2020)

Peaks for all AMPs often occur at 0h, 18h, 30, 36 and 42h after WP stage. As mentioned before, Gce seems to be crucial for downregulation during the WP stage while the same seems to be the case for Met at 36h. in the *y w* genotype all AMPs reach their highest expression at 18h after WP stage. During WP stage lysis of the larval tissue begins and ecdysone is active. (Jiang, et al., 1997) 18h after WP stage, lysis continues, the Malpighian tubules migrate, and legs and wings extend. (Jiang, et al., 1997) (Tyler, 2000) 30, 36 and 42h after WP stage Malpighian tubules turn green and the yellow body appears. (Tyler, 2000) Especially lysis of tissue and abdominal reconstruction included yellow body formation are likely candidates for triggering an immune response. JH signaling could have the same molecular trigger role found for reproduction and immunity during metamorphosis, this time suppressing immunity in favor of developmental events and against autoimmunity. (Schwenke & Lazzaro, 2017)

It has been previously found that ecdysone plays a big role in regulating metamorphosis and AMP expression. (Jiang, et al., 1997) Both ecdysone and JH have been found to regulate immunity. (Jiang, et al., 1997) (Jindra, et al., 2015) To better understand the role of JH and its receptors it may be interesting to investigate the correlation between JH and ecdysone during metamorphosis.

Effect of artificial JH on AMP mRNA expression

In this experiment the direct effect of a JHa, PRX, on each AMP in the control group and in the mutant JH receptor background was investigated. Comparing the results within and in between genotypes indicate the role and importance of the JH receptor. The effect and strength JHa has on each AMP is diverse, but the overall effect of PRX being an immune suppressor could be observed, mainly in the *y w* genotype.

My findings:

When focusing on the 3 different genotypes it stands out that in the wildtype-like genotype all AMPs show reduced expression after PRX treatment. In *y w*, Def is reduced by 88%, which is the strongest effect of JHa among the investigated AMPs. When Gce is missing, treatment with PRX does not reduce expression of Dro and Att-D. Def and CecA are still suppressed upon PRX application, while Att-A, Dpt and MTK even show upregulation in the samples treated with PRX. In the absence of the JH receptor Met, PRX is still able to downregulate Dpt, Def, CecA, Att-D and Att-A, but Dro and especially MTK show increased expression.

Comparison of the results with data from different sources

The data shown in figure 59 were obtained from previous experiments similar to the setup of the experiment in this thesis. The data provided by Marek Jindra was not published. The significant suppression of Att-A at 18h after treatment with PRX matches my result of an 72% downregulation of this AMP 18h after WP stage upon PRX application.
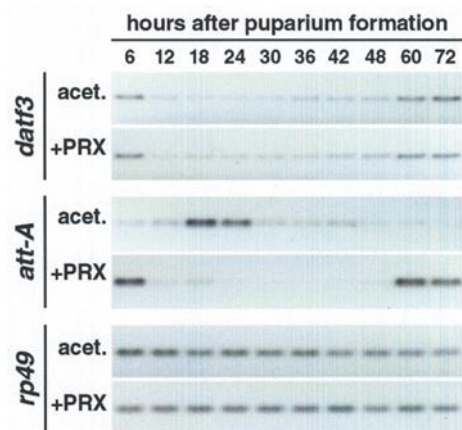
Figure 59: expression profiles of datf3, Att-A and RP49 after treatment with PRX and in an acetone treated control group

In a previous study it was detected that Defensin was only slight suppressed after JH III treatment, then Attacin D, Drosocin, Metchnikowin and Cecropin A1 followed in this order, with Diptericin being highly suppressed. (Flatt, et al., 2008) My results show a high suppression of Def after PRX treatment, while the results for Att-D, Dro and Dpt match and CecA and MTK suppression are very. The discrepancy in Def downregulation could be explained by the developmental stage. Flatt et al. worked with adult flies while I used pupae in the middle of metamorphosis. This could be further proof that Def has a developmental role during metamorphosis. (FlyBase, 2020)

With Met silenced, JHa Methoprene and JH III was found to still fully suppressed Dpt activity. (Flatt, et al., 2008) In my experiment the null allele Met^{27} did not stop PRX to slightly suppress Dpt.

In adult flies Schwenke and Lazzaro found that treatment with Methoprene suppressed DptA, MTK, Def, AttA and CecA. (Schwenke & Lazzaro, 2017) Flatt et al. similarly found Dro and Dpt suppression after treatment with Methoprene. (Flatt, et al., 2008) In my results all AMPs were suppressed after PRX application in the *y w* background as well.

JH and JH receptor effect

At 18h after pupation a high expression of AMPs can be seen in all 3 genotypes, with the AMPs even reaching their highest natural expression in the wildtype-like genotype in this stage. This could be caused by a natural upregulation after immune challenge in this stage. Treating WP with JH should downregulate the expression of AMPs and the peaks should be lowered in comparison to pupae with no prior JH treatment.

JH and JH analogs like PRX downregulate the expression of AMPs. (Flatt, et al., 2008) (Jindra, et al., 2015) (Schwenke & Lazzaro, 2017) The suppression of all AMP genes investigated in this thesis after PRX treatment confirms this statement.

JH signalling mediated by *gce* suppresses Att-D and Dro, which explains the lack of suppression after PRX treatment in the *w gce*[2,5k] background. Dpt, Def, CecA, Att-D and Att-A were still suppressed by PRX with Met missing, indicating that either functional Gce is a sufficient substitute or that Met is not involved in the JH signalling that suppresses these AMPs. Def and CecA are still suppressed in the absence of Gce or Met, respectively, a probable explanation being that for these AMPs they can substitute each other.

Rather surprisingly, Att-A, Dpt and MTK were induced by PRX in the absence of Gce and the expression of MTK and Dro was increased after PRX treatment in *w Met*[27]. If JH signalling functions correctly over Gce or Met mediation, AMP expression levels would rise when Gce or Met are missing. To follow that line of thought, when Gce and Met are missing as mediators and JH cannot exert its function over these receptors, addition of PRX, a JHa, should not be influencing AMP expression as well, the AMP expression levels should not change much in comparison to Gce and Met missing and no PRX treatment. But in these samples, AMP expression increased upon treatment with PRX. Some genes are induced rather than suppressed by JH, as Flatt et al. suggested, but if this effect occurs when Gce or Met is missing, the effect might not be mediated over these JH receptors. (Flatt, et al., 2008)

Conclusion

The hypothesis we started this thesis with was confirmed to a large extent. The prevailing trend of immune gene upregulation in the absence of JH signaling, particularly in the genotype *w gce*[2,5k] lacking a functional Gce receptor, and in some cases downregulation by JHa, indicate the immune suppressive function of JH during metamorphosis mainly mediated by Gce. The results show clearly, that not all the AMP genes follow the same trend, which may reflect their different and more complicated regulation.

Lowered AMP expression (downregulation) means the AMP gene is sensitive to the loss of this receptor. Increased AMP expression (upregulation) in a mutated JH receptor background indicates an immune response without a functioning JH receptor, probably because the AMP is suppressed over this JH receptor.

Some genes are more sensitive to the loss of the JH receptor Met, some more sensitive to the loss of Gce. The results show that Drosocin and Attacin A and D are regulated by JH signalling mediated by Gce. Cecropin A, Defensin, Diptericin, Metchnikowin react to both Met and Gce, indicating that regarding these AMPs Met and Gce can be substituted with JH signalling still being functional.

In several timepoints during metamorphosis regulation of AMP expression and therefore immune suppression by JH and its receptors Gce and Met could be detected. Especially high regulation by JH can be observed in the white puparium stage and 36h after this stage correlating with lysis and abdominal restructuring events during metamorphosis.

Figures

References

Bainbridge, S. P. & Bownes, M., 1981. Staging the metamorphosis of Drosophila melanogaster. *J. Embryol. exp. Morph. Vol. 66*, pp. 57-80.

Flatt, T. et al., 2008. Hormonal regulation of the innate immune response in Drosophila melanogaster. *The Journal of experimental Biology*, 3 June, pp. 2712-2724.

Flybase, 2020. *Allele:Dmel\gce2,5k.* [Online]
Available at: https://flybase.org/reports/FBal0266011
[Zugriff am 5 May 2020].

FlyBase, 2020. *Allele:Dmel\Met27.* [Online]
Available at: https://flybase.org/reports/FBal0089546
[Zugriff am 5 May 2020].

FlyBase, 2020. *Gene: Dmel/Dro.* [Online]
Available at: http://flybase.org/reports/FBgn0010388
[Zugriff am 12 May 2020].

FlyBase, 2020. *Gene: Dmel\AttA.* [Online]
Available at: http://flybase.org/reports/FBgn0012042
[Zugriff am 12 May 2020].

FlyBase, 2020. *Gene: Dmel\AttD.* [Online]
Available at: http://flybase.org/reports/FBgn0038530
[Zugriff am 12 May 2020].

FlyBase, 2020. *Gene: Dmel\CecA1.* [Online]
Available at: http://flybase.org/reports/FBgn0000276
[Zugriff am 12 May 2020].

FlyBase, 2020. *Gene: Dmel\Def.* [Online]
Available at: http://flybase.org/reports/FBgn0010385
[Zugriff am 12 May 2020].

FlyBase, 2020. *Gene: dmel\DptA.* [Online]
Available at: http://flybase.org/reports/FBgn0004240
[Zugriff am 12 May 2020].

FlyBase, 2020. *Gene: Dmel\Mtk.* [Online]
Available at: http://flybase.org/reports/FBgn0014865
[Zugriff am 12 May 2020].

Flybase, 2020. *Gene:Dmel\w.* [Online]
Available at: https://flybase.org/reports/FBgn0003996
[Zugriff am 5 May 2020].

FlyBase, 2020. *Gene:Dmel\y.* [Online]
Available at: https://flybase.org/reports/FBgn0004034
[Zugriff am 5 May 2020].

Jiang, C., Baehrecke, E. H. & Thummel, C. S., 1997. Steroid regulated programmed cell death during Drosophila metamorphosis. *Development*, 10 September, pp. 4673-4683.

Jindra, M. et al., 2015. Genetic evidence for function of the bHLH-PAS Protein Gce/Met as a juvenile hormone receptor. *PLOS Genetics*, 10 July, pp. 1-16.

NCBI, 2020. *Nucelotide.* [Online]
Available at: https://www.ncbi.nlm.nih.gov/nuccore
[Zugriff am 4 May 2020].

Schwenke, R. A. & Lazzaro, B. P., 2017. Juvenile Hormone suppresses resistance to infection in mated female Drosophila melanogaster. *Current Biology*, 20 February, pp. 1-6.

Tamone, S. L., 1997. *Identification and Characterization of Methyl Farnesoate Binding Proteins from the Crab,Cancer magister - Scientific Figure on ResearchGate. Available from:.* [Online]
Available at: https://www.researchgate.net/figure/Chemical-structures-of-insect-juvenile-hormone-III-JH-III-1-me
[Zugriff am 13 May 2020].

Tyler, M. S., 2000. *Developmental biology, A quide for experimental study.* 2. Hrsg. Sunderland, MA.: Sinauer Associates, Inc. Publishers.

University of Washington, kein Datum *The Berg Lab - An Introduction to Drosophila melanogaster.* [Online]
Available at: http://depts.washington.edu/cberglab/wordpress/outreach/an-introduction-to-fruit-flies/
[Zugriff am 15 May 2020].